Epithelial-to-mesenchymal transition in human lung epithelial cells

Hulda Rún Jónsdóttir

Thesis submitted for the degree of Master of Science
University of Iceland
Faculty of Medicine
School of Health Sciences
June 2012

HÁSKÓLI ÍSLANDS

Bandvefsumbreyting í mennskum lungnaþekjufrumum

Hulda Rún Jónsdóttir

Ritgerð til meistaragráðu í líf- og læknavísindum

Umsjónarkennari: Þórarinn Guðjónsson

Leiðbeinandi: Magnús Karl Magnússon

Meðleiðbeinandi: Sigríður Rut Franzdóttir

Meistaranámsnefnd: Magnús Karl Magnússon og Tómas Guðbjartsson

Lífvísindasetur

Læknadeild

Heilbrigðisvísindasvið

Háskóli Íslands

Júní 2012

Epithelial-to-mesenchymal transition in human lung epithelial cells

Hulda Rún Jónsdóttir

Thesis sumbitted for the degree of Master of Science

Supervisors: Þórarinn Guðjónsson and Magnús Karl Magnússon

Co-supervisor: Sigríður Rut Franzdóttir

Masters comitte: Magnús Karl Magnússon og Tómas Guðbjartsson

Biomedical Center

Faculty of Medicine

School of Health Sciences

University of Iceland

June 2012

Háskólaprent

Reykjavík, Ísland 2012

Ágrip

Lungnatrefjun af óþekktum uppruna (e. idiopathic pulmonary fibrosis, IPF) er alvarlegur lungnasjúkdómur sem felur í sér aukna myndun bandvefs. Uppruni þessara bandvefsfruma er ekki þekktur en talið er að bandvefsumbreyting þekjufruma (e. epithelial-to-mesenchymal transition, EMT) geti stuðlað að vefjatrefjun í ýmsum líffærum og þ.m.t lungnatrefjun. EMT er þekkt ferli við miðlagsmyndun í fósturþroska og er einnig nauðsynlegt við myndun greinóttra líffæra þar sem þekjuvefsfrumur skríða inn í aðlægan bandvef. Bandvefsumbreyting hefur einnig verið tengd ífarandi krabbameinsvexti þar sem æxlisfrumur úr þekjuvef missa þekjuvefseinkenni sín, öðlast aukna skriðhæfileika og verða að ífarandi æxlisfrumum. Mikilvægt er að öðlast aukna þekkingu á EMT í lungum og þá sérstaklega í tengslum við IPF þar sem slíkt gæti varpað ljósi á tilurð þessa illvíga sjúkdóms og stuðlað að þróun nýrra og betri meðferðarúrræða.

Markmið verkefnisins var að skoða svipgerðareiginleika lungnaþekjufruma í eðlilegum lungnavef, lungnavef úr IPF sjúklingum og í frumurækt með tilliti til getu lungnaþekjufruma til að undirgangast EMT

Þegar vefjasýni úr lungum með IPF voru borin saman við heilbrigð viðmiðunarsýni sást aukin tjáning á Vimentin og CK14 í þekjufrumum sem lágu aðlægt svæðum með lungnatrefjun (e. fibroblastic foci). Þetta bendir til þess að þekjuvefsfrumurnar hafi hugsanlega undirgengist EMT og vekur upp spurningar hvort trefjuð svæði geti átt uppruna sinn í aðlægri lungnaþekju.

Til þess að meta hvort lungnaþekjufrumur í rækt gætu undirgengist EMT var VA10 lungnaþekjufrumulínunni komið fyrir í ræktunarskilyrðum sem fela í sér meðhöndlun með sermisígildinu Ultroser G sem ýtir undir frumusérhæfingu. Eftir meðhöndlun varð greinileg svipgerðarbreyting á undirhópi fruma innan VA10 en þessar frumur verða ílangar og bandvefsfrumulíkar. Frumurnar sýndu minnkaða tjáningu þekjuvefspróteina og aukningu í tjáningu bandvefskenniþróteina. Eftir aðskilnað gátu þessar bandvefslíku frumur ekki lengur myndað greinótta formgerð í þrívíðum ræktum líkt og venjulegar VA10 frumur. Þær sýndu einnig aukið skrið og aukinn vöxt í mjúkagar sem staðfestir að þessar frumur hafi áunnið sér bandvefsfrumureiginleika. Til að staðfesta frekar að þessar sömu frumur hafi undirgengist EMT var tjáning microRNA 200c metin en tjáning miR200c er bæld í frumum sem hafa undirgengist EMT. Það reyndist einnig vera raunin í bandvefslíkum VA10 frumum.

Í framhaldi var einnig kannað hvort hægt væri að valda EMT í eðlilegum lungnaþekjufrumum einangruðum úr ferskum vef. Í því sambandi voru settar upp aðferðir til einangrunar og ræktunar á ferskum lungnaþekjufrumum. Fyrstu niðurstöður benda til þess að ekki sé hægt að valda EMT með Ultroser G meðhöndlun í ferskum frumum. Þetta bendir til þess að eðlilegar frumur úr vef séu ekki eins sveiganlegar m.t.t svipgerðarbreytingar eins og ódauðlegar frumulínur.

Þessi rannsókn hefur gefið vísbendingar um að orsök IPF sé að hluta til bandvefsumbreyting þekjuvefsfruma. Nauðsynlegt er að gera frekari rannsóknir á vefjasýnum til þess að kanna umfang EMT í stærra þýði IPF sjúklinga. Einnig er mikilvægt að ákvarða hvaða þættir í Ultroser G ræktunarætinu valda EMT í VA10 frumulínunni.

Abstract

Idiopathic pulmonary fibrosis (IPF) is a severe lung disease with high morbidity and mortality. The cellular source of IPF is currently unknown but one suggested source is epithelial-to-mesenchymal transition (EMT). EMT is a well defined process in embryonic development and is absolutely essential for the formation of branching organs where epithelial cells must migrate into the surrounding stroma. EMT has also been related to various pathological situations such as invasive and metastatic cancer growth. The connection of EMT to IPF has only recently been suggested and further studies are needed to confirm the different cellular processes in this disease.

The aim of this study was to evaluate the phenotype of normal lung tissue, tissue from patients suffering from IPF and the plasticity of lung epithelial cells in culture, emphasizing their ability to undergo EMT.

In this study, lung samples from patients with IPF were compared to normal reference samples. Marked increase in both Vimentin and CK14 expression was observed in epithelium adjacent to fibrotic areas (fibroblastic foci). This could indicate that cells within the epithelium have undergone partial EMT and might somehow be contributing to the fibrotic conditions in IPF.

To support these *in situ* studies experiments were also conducted on an immortalized human bronchial epithelial cell line, referred to as VA10. VA10 cells were treated with the serum substitute Ultroser G. After treatment, morphological changes were observed in a subset of cells. These cells lose their epithelial phenotype and become elongated and mesenchymal-like. The cells also lose expression of known epithelial surface markers and gain a more mesenchymal expression profile. After sorting, these mesenchymal-like cells can no longer undergo branching morphogenesis, one of the characteristics of the original VA10 cell line. Additionally, these cells show increased potential for migration and anchorage independent growth further confirming their mesenchymal traits. To further confirm that this change in morphology and marker expression was, in fact, caused by EMT the expression of microRNA 200c was assessed. The expression of miR200c has been shown to be down regulated in cells that have undergone EMT and it is also downregulated in mesenchymal-like VA10 cells.

In order to be able to analyze whether primary bronchial cells could undergo EMT when treated with Ultroser G protocols for the isolation and culture of primary bronchial cells from fresh lung tissue were established. Initial studies indicate that primary cells are not as prone to EMT as our cell line model. This indicates that normal primary cells do not exhibit the same level of plasticity as an immortalized cell line.

This study indicates that IPF is partly caused by EMT in pulmonary epithelial cells. It is, however, necessary to properly evaluate the involvement of EMT in IPF by analyzing more IPF patient samples. Additionally, it is very important to determine what factors within Ultroser G are responsible for EMT induction in VA10 cells.

Acknowledgements

This work was carried out at the Stem Cell Research Unit, Biomedical Center, University of Iceland and Department of Laboratory Hematology, Landspítali.

I would like to take this opportunity and thank those who have contributed to the project.

First of all I would like to thank my supervisors **Dr. Þórarinn Guðjónsson**, **Dr. Magnús Karl Magnússon, MD** and **Dr. Sigríður Rut Franzdóttir** for giving me the opportunity to work on this project. Their enthusiasm and passion for science has been a true inspiration to me.

I would also like to sincerely thank all my friends and colleagues at the Stem Cell Research Unit, Landspítali and Biomedical Center for providing a stimulating and entertaining work environment. I would especially like to thank **Ari Jón Arason** for all his help during my first months at the laboratory and his continued help and guidance through the remainder of this project. I would also like to thank **Sævar Ingþórsson**, **Bylgja Hilmarsdóttir**, **Berglind Eva Benediktsdóttir, Dr. Jón Þór Bergþórsson** and **Dr. Valgarður Sigurðsson** for their invaluable companionship, help and support.

I would also like to acknowledge the following individuals:
Dr. Hekla Sigmundsdóttir, Þórdís Emma Stefánsdóttir and **Íris Pétursdóttir** at the Department of Laboratory Hematology for their assistance and expert advice on flow cytometry.

Dr. Tómas Guðbjartsson, MD, a member of my MS-committee, for his valuable collaboration regarding isolation of primary lung cells from human tissue. I also thank him for good advice during the writing of this thesis.

Dr. Ólafur Baldursson, MD PhD for his involvement in this and other lung related projects conducted at our laboratory.

Dr. Ragnar Pálsson, MD, **Dr. Gunnar Guðmundsson, MD**, **Dr. Helgi Ísaksson**, **MD** and **Kristrún Auður Ólafsdóttir** at the Department of Pathology, Landspítali for their collaboration on the IPF part of this project.

Last but not least, I would like to thank my friends and family for all their support and encouragement during my studies. I would especially like to thank my love **Arnar M. Ellertsson** for his patience and understanding.

This project was supported by the Icelandic Research Council, University of Iceland Science Fund, Landspítali Science Fund and the Student Innovation Fund.

Table of Contents

List of Figures

List of Tables

Abbreviations

2D	Two-dimensional
3D	Three-dimensional
ALI	Air Liquid Interface
BSA	Bovine Serum Albumin
cDNA	Complementary DNA
CK	Cytokeratin
CPT	Camptothecin
DMEM	Dulbecco's Modified Eagles Medium
ECM	Extracellular Matrix
EDTA	EthyleneDiamineTetraacetic Acid
EMT	Epithelial-to-Mesenchymal Transition
EpCAM	Epithelial Cell Adhesion Molecule
FBS	Fetal Bovine Serum
FGF	Fibroblast Growth Factor
FGFR	Fibroblast Growth Factor Receptor
GAPDH	GlycerAldehyde 3-Phosphate DeHydrogenase
HPV	Human Papilloma Virus
HUVECs	Human Umbilical Vein Endothelial Cells
IL	Interleukin
IPF	Idiopathic Pulmonary Fibrosis
IR	Infrared
MACS	Magnetic Cell Sorting
miRNA	Micro RNA
OD	Optical Density
PBS	Phosphate Buffered Saline
PCR	Polymerase Chain Reaction
PVDF	Polyvinylidene Fluoride
qRT-PCR	Quantitative Real-Time PCR
rBM	Reconstituted Basement Membrane
RIPA	Radioimmunoprecipitation
RPM	Rotations Per Minute
SMG	SubMucosal Gland
TBS	Tris Buffered Saline
TE	Tris-EDTA
UG	Ultroser G

I – Introduction

1. Lung Development

The lungs are a derivative of the fetal digestive tube and develop by extension of the laryngotracheal groove. This groove splits into two branches that eventually form the bifurcated bronchi. The endoderm of the laryngotrachea then becomes the epithelial lining of the mature lungs. Branching morphogenesis of this endodermal tube, to yield the alveoli, is tightly regulated by mesodermal cells in the immediate surroundings (Gilbert, 1997).

Branching morphogenesis is a conserved developmental process and is observed in the development of several tubular organs such as lungs, kidneys and breasts. These organs develop in a hierarchical manner where a single major conduit elaborates gradually into thinner conduits eventually terminating in conduits only made up of a single cell layer (figure 1). The lumina of such complex systems are composed of either endothelial or epithelial cells. When it comes to the vascular and lymphatic systems they are made of endothelial cells while lumina in all other human systems are comprised of epithelial cells. The general morphology of tubular systems is determined by the angle between new branches, as well as their number (reviewed in (Horowitz & Simons, 2008)).

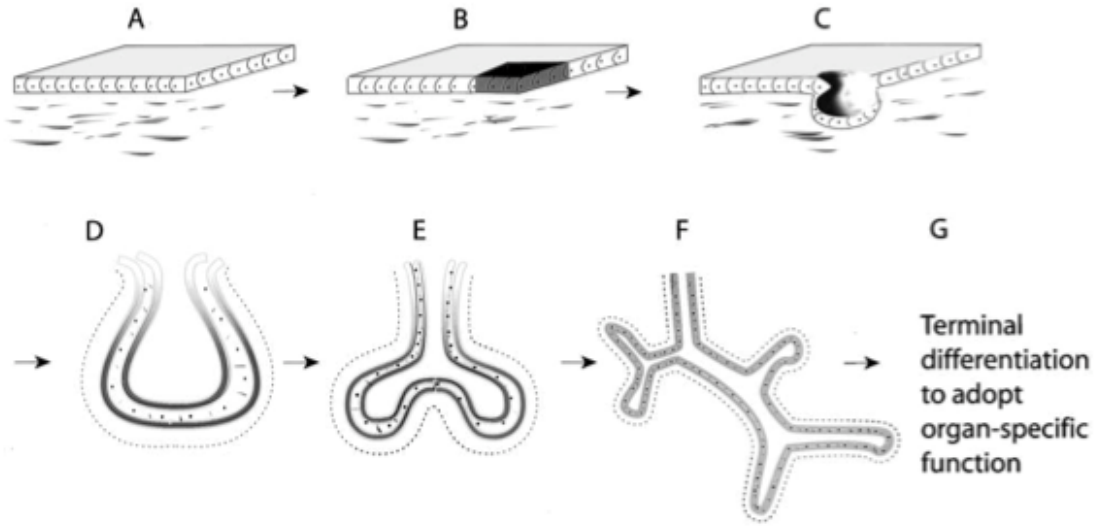

Figure 1: Branching morphogenesis. During the initiation of branching morphogenesis on a cellular level a subset of cells (dark patch in **B**) of the epithelium **(A)** is instructed to undergo branching morphogenesis. The cells migrate outwards from the epithelial layer **(C)** and progress into budding **(D)**, bifurcation **(E)** and branching **(F)**. The resulting branching structure then undergoes terminal differentiation and adopts it's organ specific function **(G)** (Affolter et al., 2003).

In humans, the lungs form around the 5th week of gestation from the laryngotracheal groove in the endodermal epithelium. Branching morphogenesis occurs prenatally and is typically over by the 16th week. Alveolarization starts at around 20 weeks of gestation and is concluded postnatally (Warburton et al., 2000). The lungs are one of the last mammalian organs to complete their differentiation since their function is not required until after birth. In order to keep the alveolar sacs from collapsing and interfering with gas-exchange the alveolar cells secrete surfactant into the fluid lining the lungs. The level of surfactant usually reaches useful levels around week 34 in the human fetus. Infants born prematurely often have difficulty breathing due to insufficient surfactant production (Gilbert, 1997). The complex branching of the alveoli is accompanied by the development of the pulmonary vasculature. Close contact between the alveoli and vasculature is needed in order to produce a functioning gas exchange system (figure 2) (Shannon & Hyatt, 2004).

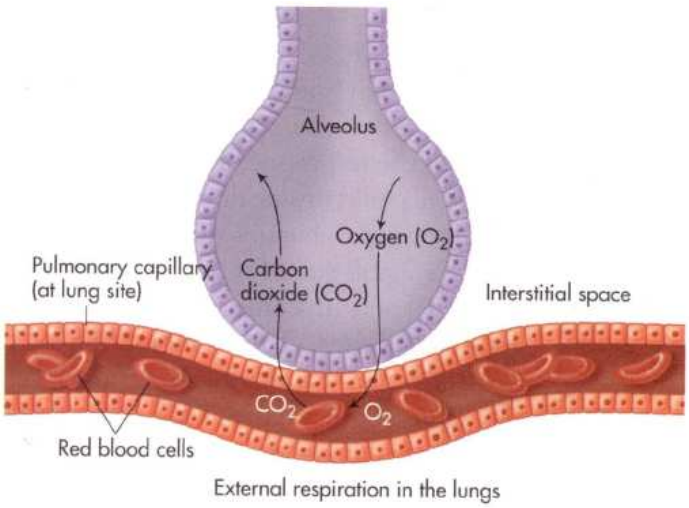

Figure 2: Pulmonary gas exchange. Alveoli are in close contact with the pulmonary vasculature to facilitate external respiration. Carbon dioxide is expelled from the body while red blood cells are replenished with fresh oxygen (Colbert et al., 2009).

2. Lung histology

The human lung is a complex organ that spans a relatively long anatomical distance. The lungs are composed of complex tubular networks with the predominant function to manage the body's gas exchange. Although, different areas of the lungs are composed of different cells with various roles in lubrication, host-defense and maintenance. The upper airways are often termed conducting airways and they terminate in roughly 2^{17} terminal bronchioles, which in turn give rise to 6 generations of alveolar ducts each. These alveolar ducts terminate in the alveolar sacs that are responsible for the actual gas exchange (figure 2) (Mauroy et al., 2004). The lungs also incorporate other passages, the extrapulmonary passages, which reside outside the lung tissue itself. These passages include the larger bronchioles, bronchi and trachea. The extrapulmonary passages are lined with ciliated pseudostratified epithelium that contains a number of goblet and neuroendocrine cells. As discussed in the next chapter, the pseudostratified epithelium is maintained by basal cells that reside on the basal membrane. As these passages enter the lungs their conduits become narrower resulting in a gradual loss of cilia and goblet cells. In addition, the height of the epithelial layer also decreases. Down in the alveolar sacs the epithelial layer is no longer pseudostratified and goblet cells are no longer found. The epithelium lining the alveoli is classified as simple squamous epithelium in contrast to the pseudostratified epithelium in the conducting airways (Eroschenko, 2005).

3. Lung stem cells

Most tissues are maintained by tissue specific somatic stem cells. This is portrayed the clearest in epithelial tissues with rapid cellular turnover, such as the skin and colon (Lipkin et al., 1962; Weinstein et al., 1984). The general rate of cell turnover differs between the various tissues of the body. For example, epithelial cell turnover in the lungs can take up to 6 months under normal conditions (Pellettieri & Sanchez Alvarado, 2007) compared to several days/weeks in the human skin. When confronted with tissue damage or chronic injury the cell turnover rate in the lungs rapidly increases to replenish damaged tissue (Giangreco et al., 2009).

Somatic stem cells are defined by their ability to divide asymmetrically, thereby creating differentiated progeny as well as renewing themselves (figure 3). Regulation of asymmetric cell division is imperative for normal tissue homeostasis. Loss of this regulation is believed to have a role in the earliest stages of carcinogenesis (Chang et al., 2012; Gudjonsson & Magnusson, 2005).

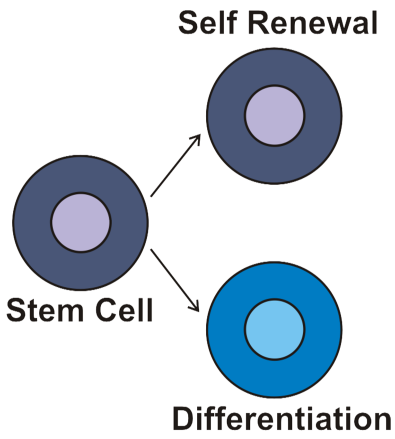

Figure 3: Asymmetric cell division. When stem cells divide asymmetrically they renew themselves as well as producing differentiated progeny.

It has proven difficult to evaluate and isolate distinct stem/progenitor cells from human lung tissue mainly due to the complexity of the lung epithelium, which contains many morphologically distinct epithelial cells. In addition, lack of normal human lung tissue for research along with difficulties with both isolation and culture of primary lung epithelial cells make cell isolation even more difficult.

Since different areas of the lungs possess different functional abilities these different areas have been proposed to possess distinct stem cell niches. Therefore, various cells with stem cell properties have been identified in the adult lung (Kotton & Fine, 2008). In the upper airways, a few CK14 positive basal cells along with Clara cells and cells within submucosal glands are believed to be responsible for replenishing the bronchial epithelium (Giangreco et al., 2007; Hong et al., 2004; Kotton et al., 2008). In the alveoli, the alveolar type II epithelial cells are perceived to be a progenitor cell in the alveolar epithelium due to its ability to regenerate itself as well as giving rise to alveolar type I epithelial cells. Additionally, neuroendocrine cells that reside in neuroepithelial bodies within the lung tissue have been reported to play a role in the regeneration of pulmonary epithelium after lung injury (Reynolds et al., 2000). This indicates both progenitor cell capabilities and plasticity of different types of lung epithelial cells.

So far, no single somatic stem cell type capable of replenishing both proximal and distal lung epithelial cells has been described (Kotton et al., 2008).

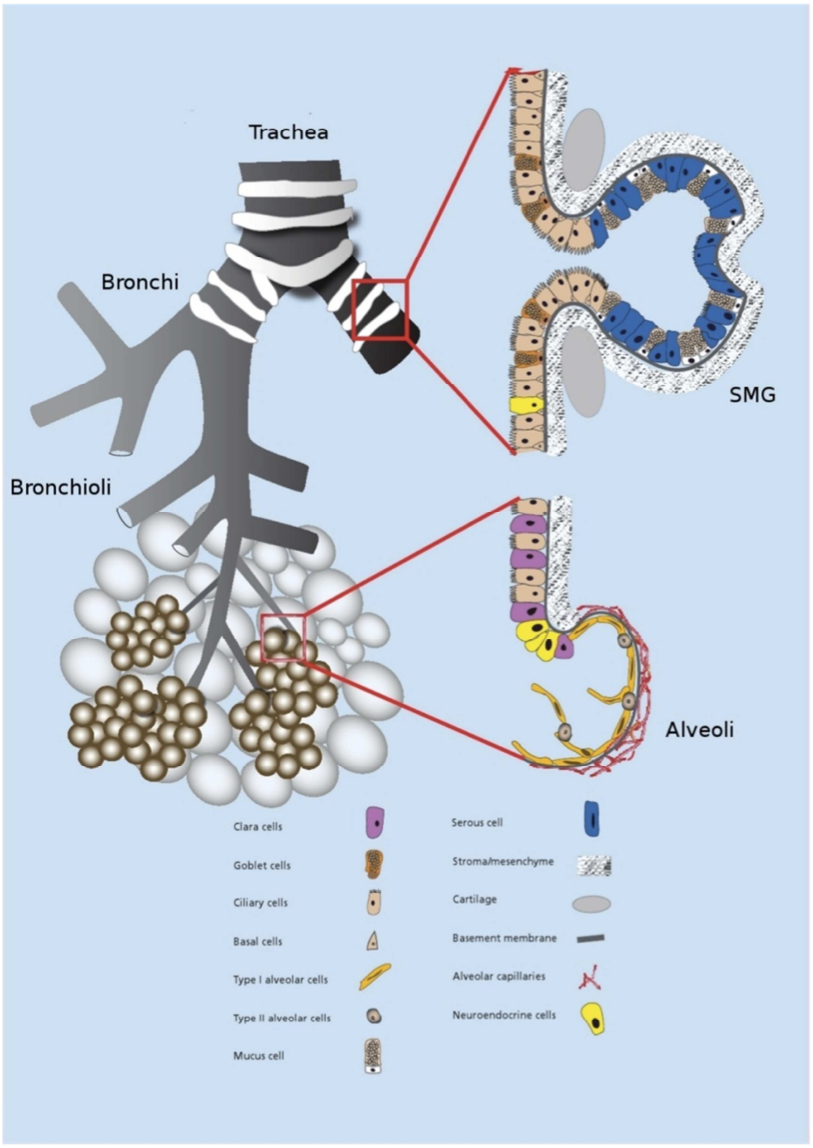

Figure 4: Lung anatomy is complex. The lung is a large and complex organ with a variety of functions. Many different cell types with different functions are found in the human lung. For example, ciliated cells (tan) are responsible for getting rid of debris while goblet cells (brown) secrete protective mucus. The lungs contain various progenitor cells, the basal cells (small tan) and Clara cells (purple) in the upper conducting airways, neuroendocrine (yellow) cells in the broncioalveolar junction and alveolar type II cells in the alveoli (round tan) (Magnusson & Gudjonsson, 2011).

Most studies on lung development and lung stem cells have been conducted in the murine system since it is ultimately more difficult to conduct these experiments in humans. However, there is a substantial and important structural and functional difference between the various cell types and their function when mouse lungs are compared to human. This results in a somewhat two-sided literature since murine observations cannot be directly transferred and translated to the human system (Shapiro, 2006; Ware, 2008).

Even though the epithelial cells are the functioning unit of the respiratory system they are largely dependent on interactions with the surrounding stroma.

4. Epithelial – stromal interactions

The lung epithelium is surrounded by tissue specific mesenchyme, commonly referred to as stroma, containing various stromal cell types. These cells include endothelial cells, cells of the immune system and fibroblasts. Fibroblasts secrete extracellular matrix (ECM) proteins and growth factors into the mesenchyme in order to maintain organ functionality and order (Pageau et al., 2011). Stromal cells have multiple roles in both normal lung development as well as in the pathogenesis of disease. For example, the endothelial cells surrounding the alveoli of the lungs are crucial for successful air-exchange (Maeda et al., 2002). However, many pulmonary diseases are believed to be a result of altered communication between lung epithelial cells and the surrounding mesenchyme (Pageau et al., 2011).

During normal lung morphogenesis, epithelial-stromal interactions are imperative for initial branching induction (Shannon et al., 2004). Dr. Dorothea Rudnick first established the importance of lung epithelial-stromal interactions about 80 years ago. She demonstrated that chick lung development arrested when the lung mesenchyme was removed from the cultures (Demayo et al., 2002; Rudnick, 1933).

In 1994, Shannon et al. demonstrated that the tracheal epithelium of a rat fetus could be reprogrammed by exposing it to distal lung mesenchyme to create a lung-like branching pattern and the distal lung cell phenotype of alveolar type II cells (Shannon, 1994). In addition, four years later Shannon et al. also showed that rat tracheal epithelium could be reprogrammed into various lung cell types, all depending on the type of mesenchyme it was exposed to (Shannon et al., 1998). This clearly demonstrates the importance of epithelial-stromal interactions during lung organogenesis and the plasticity of lung epithelial cells to respond to changes in the microenvironment found within the interactive mesenchyme.

Epithelial-stromal interactions are also important when it comes to understanding certain pathological situations in the lung, such as pulmonary cancer and fibrosis. Factors secreted by an unbalanced or diseased mesenchyme can influence surrounding epithelial cells and create a state of illness. Epithelial-to-mesenchymal transition is one of the processes induced by secreted factors from the mesenchyme (reviewed in (Moustakas & Heldin, 2007)).

5. Epithelial-to-mesenchymal transition (EMT)

Epithelial-to-mesenchymal transition (EMT) is a process well known in normal development. In embryonic development EMT is crucial for mesoderm formation and the migration of neural crest cells from the neural tube to various sites within the embryo (figure 5) (Kerosuo & Bronner-Fraser, 2012; Savagner, 2010). Additionally, EMT plays a role in wound healing in the skin allowing repairing cells to gain migratory potential (Nakamura & Tokura, 2011).

Organogenesis depends largely on EMT and its reversible counterpart mesenchymal-to-epithelial transition (MET). In development these processes are interchangeable and it usually takes several rounds of EMT and MET to achieve a complex three-dimensional organ structure. Additionally, EMT has been found to play a role in various diseases, most prominently in cancer and fibrosis (reviewed in (Thiery et al., 2009)). In cancer, EMT is critical both for invasiveness and metastasis.

The initiation of EMT is marked by repression of the epithelial cell adhesion molecule E-cadherin and the dissociation of the epithelial cells. The epithelial cells lose their distinct marker expression and gain a more mesenchymal expression profile. This expressional switch includes an increase in the expression of various mesenchymal markers, such as Vimentin, N-cadherin and Fibronectin (Mongroo & Rustgi, 2010).

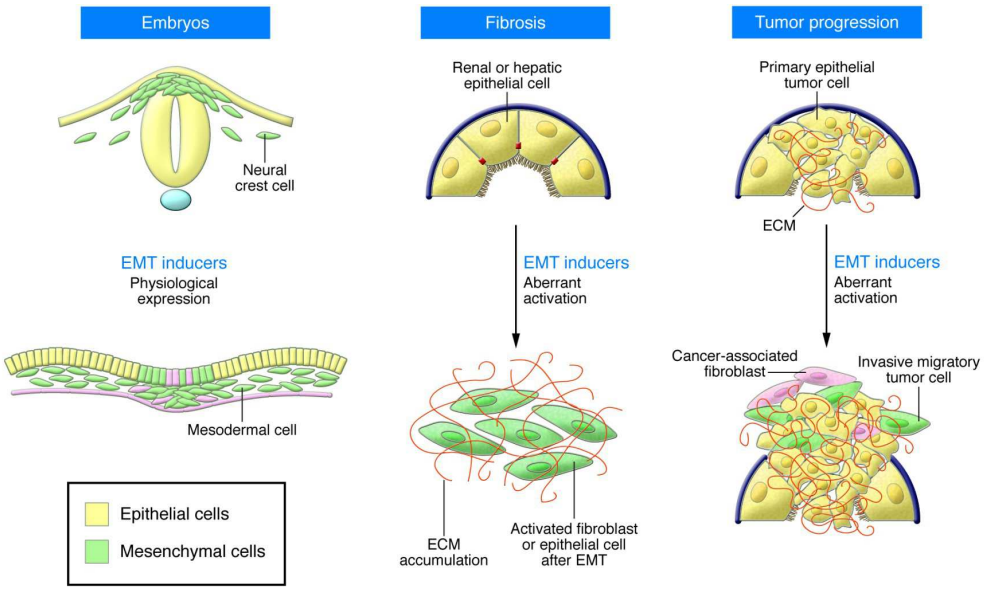

Figure 5: Epithelial-to-mesenchymal transition in normal development and disease. EMT is critical for various processes in normal development. Including neural crest formation in the embryo. Additionally, it can play a part in pathogenesis of various diseases. In fibrosis, EMT is induced and the epithelial cells gain a mesenchymal phenotype. Accumulation of extracellular matrix (ECM) contributes to fibrotic conditions. In cancer, EMT is induced in tumor cells that, in turn, gain a migratory potential and become both invasive and metastatic (reviewed in (Acloque et al., 2009)).

5.2 Idiopathic pulmonary fibrosis (IPF)

Idiopathic pulmonary fibrosis (IPF) is a severe medical condition characterized by scarring and thickening of the lung tissue within characteristic fibroblastic foci that are found in close proximity to the lung epithelium. These foci will eventually lead to a loss of function in the surrounding pulmonary epithelium followed by severe respiratory failure. IPF is quite difficult to diagnose but it has been indicated that surgical lung biopsies serve as the optimal diagnostic procedure when dealing with complex interstitial lung diseases (M. I. Sigurdsson et al., 2009). Recent studies have also suggested a direct correlation between the number of fibroblastic foci assessed by surgical biopsy and survival and physiologic deterioration of patients (reviewed in (Hardie et al., 2010)). Few unique treatment options are available for these patients but general treatment includes anti-inflammatory drugs and steroids (reviewed in (Hardie et al., 2010)).

Many different cellular sources have been suggested for these characteristic foci but mainly three theories have persisted. Firstly, people have speculated that these fibroblastic cells are resident fibroblasts/myofibroblasts from the lung. The second theory revolves around mesenchymal stem cells from the blood that have taken residence within the lung tissue. The last and latest theory states that the cells within the foci are lung epithelial cells that have undergone EMT and gained a mesenchymal phenotype (Willis et al., 2006).

Recently, studies have shown that various microRNAs (miRNAs), predominantly the miR200 family, play an important role in both EMT and lung fibrosis (Eades et al., 2011; Yang et al., 2012). miRNAs are small non-coding RNAs that regulate gene expression. These RNAs are evolutionary conserved and regulate their target genes by promoting mRNA degradation or by translational inhibition. Over the last 15 years miRNAs have been implicated in various rudimentary cellular processes such as proliferation and differentiation. Additionally, the role of miRNAs in disease is steadily emerging (Mendell & Olson, 2012).

The miR200 family members, miR200a, 200b, 200c, 141 and 429, are severely reduced in cells that have undergone TGFβ-1 induced EMT (Mongroo et al., 2010). miRNA 200c is believed to be pivotal when it comes to the down-regulation of E-cadherin, one of the hallmarks of EMT. When this miRNA is down regulated its target, the transcription factor ZEB1, is free to down-regulate E-cadherin expression (Korpal et al., 2008). This specific miRNA down-regulation is not limited to EMT induced by TGFβ-1. Breast stem cells that have undergone TGFβ-1 independent endothelial induced EMT exhibit the same pattern of down-regulation (Hilmarsdottir et al. unpublished data).

Research progress in lung development and lung diseases has benefitted greatly from studies conducted in various rodents. Due to the difference between human and rodent lung anatomy, however, researchers require human material. It is important to study both primary cells and established cell lines in the context of lung development and disease progression.

6. Lung epithelial cells in culture

To be able to study and understand human lung morphogenesis, access to representative culture models is essential. In that context, well-defined cell lines that imitate *in vivo* situations are of specific importance. In recent years, there has been limited access to cell lines established from normal human lung tissue although the number of commercially available cell lines steadily increases (table 1). In addition, the culture of primary cells isolated from human tissue becomes increasingly important due to their closeness to the tissue of origin (Pezzulo et al., 2011).

6.1 Primary cultures

Primary cultures can give a more detailed insight into *in vivo* situations since they have not been altered to grow indefinitely in culture. However, when dealing with cells from normal tissue the largest limitation is the short life span of normal somatic cells in culture due to telomere shortening followed by crisis and senescence of cultured cells. This severely inhibits the number of available investigative assays. In addition, difference between tissue donors severely limits the reproducibility of obtained results (Zabner et al., 2003). Additionally, it is unclear which cell types survive on the monolayer surface. Despite their limitations, primary cultures can address topics that cell lines are unsuitable for.

Most importantly, primary cells are closer to the tissue of origin providing a non-altered representative of *in vivo* conditions. Therefore, it is important to run parallel research on primary cells and cell lines and allow these different models to complement each other.

6.2. Cell lines

Immortalized cell lines have their limitations much like primary cells; their main handicap is possible loss of original morphology and function (Zabner et al., 2003). Although, various pulmonary cell lines with different properties are available. For example, the A549 cell line is a tumor cell line established from human alveolar adenocarcinoma. The cells seem to have a clonal origin, originating from one single cell. A549 cells are epithelioid in shape and contain clearly visible granules characteristic of alveolar type II cells. The cells also secrete surfactant, which further confirms their cellular origin. The A549 cell line was established in 1973 and has been continuously propagated since (Lieber et al., 1976). This cell line is widely used and highly cited. However, due to its carcinogenic origin it may not be the best representative for studies aimed at understanding the various roles of non-cancerous lung tissue.

Other cell lines from both normal and cancerous tissue remain available (table 1), although cell lines from cancers are more common and usually easier to grow.

Another example of a widely used cell line is Calu3. Calu3 is derived from normal human submucosal grand. When these cells are cultured in ALI cultures (described in chapter 6.3.3) they exhibit some characteristics of bronchial epithelium. Due to its cellular origin the Calu3 cell line possess different secretory potentials than alveolar epithelial cells. This cell line has been used to investigate various properties, such as drug delivery and bacterial invasiveness (Zhu et al., 2010).

Table 1: Examples of available lung cell lines from various sources[1].

Name	Origin	Cell Type	Tumorigenic
A549	Adenocarcinoma	Epithelial	Yes
Calu-3	Submucosal Gland	Epithelial	No
HEL 299	Lung Mesenchyme	Mesenchymal	No
LL 97A	Idiopathic Pulmonary Fibrosis	Mesenchymal	No
Cu-Fi 4	Cystic Fibrosis	Epithelial	No
HBE4-E6/E7-C1	Bronchus	Epithelial	No
VA10	Bronchus	Epithelial	No

A cell line derived from a normal bronchial explant was established in our laboratory by transfecting primary bronchial cells with E6 and E7 oncogenes from HPV16, using retroviral vectors. The cell line, named VA10, exhibits an epithelial cobblestone shape in monolayer culture and initial characterization demonstrated expression of CK 5/6, 13, 14 and 17. This suggests that the cell line is predominantly comprised of cells with basal cell phenotype. This was further confirmed by the expression of the basal cell associated transcription factor p63 and both the α6- and β4-integrins (Halldorsson et al., 2007). Additionally, VA10 exhibits somatic stem cell properties observed in the formation of pseudostratified epithelium in air-liquid interface cultures (described in chapter 6.3.3) (Halldorsson et al., 2007; Halldorsson et al., 2010) and bronchioalveolar branching structures when cultured in reconstituted basement membrane (Matrigel/rBM) three dimensional environment (described in chapter 6.3.2) (Franzdottir et al., 2010).

6.3 Cell culture models

6.3.1 Monolayer cultures

The most conventional way to culture cells is to simply culture them on a monolayer plastic surface (figure 6A,D). That results in a simple monolayer, or two dimensional, culture. Monolayer cultures are not well equipped to mimic organogenesis or development because the cells are not being cultured in their organotypic context. In addition, when cells are cultured on a plastic surface they tend to dedifferentiate and loose some of their specific function (Carterson et al., 2005). Monolayer cultures have proven to be important for marker expression analyses, cell proliferation, phenotypic plasticity and biochemical analyses. In order to mimic the development of branched organs one must venture outside of these traditional two-dimensional cultures.

[1] http://www.lgcstandards-atcc.org/

6.3.2 Three-dimensional cultures

Three-dimensional cultures have been developed to better capture developmental conditions and *in vivo* like histology *in vitro*. These cultures are believed to better represent various *in vivo* conditions, especially branching morphogenesis. Gel substrates are common in three-dimensional cultures and the commercially available Matrigel, produced by BD Biosciences, is a commonly used substrate. Matrigel is a reconstituted basement membrane (rBM) that contains various structural proteins such as laminin and collagen. rBMs and collagen matrices have previously been shown to induce functional differentiation and alveolar morphogenesis in primary mammary cells (Barcellos-Hoff et al., 1989; Gudjonsson et al., 2003). The cell culture model developed in our laboratory using growth factor reduced Matrigel induces branching morphogenesis in our lung epithelial cell line when the epithelial cells are co-cultured with human umbilical vein endothelial cells (HUVECs) (Franzdottir et al., 2010), further illustrating the importance of stromal cells in organogenesis. This cultures system gives a more detailed image of the development of the distal lung than traditional monolayer cultures (figure 6B,E).

6.3.3 Air-Liquid Interface (ALI) cultures

Although, three-dimensional cultures are well suited to mimic the development of the distal alveolar sacs, rBM cultures are not so well suited to mimic the condition in the upper conducting airways. In the airways, the apical side of the pseudostratified epithelium is constantly exposed to air while the basal side is resting on the basement membrane in close proximity to nutrients. In order to better simulate these specific conditions cells can be cultured in ALI cultures (figure 6C,F). In ALI cultures, cells are seeded onto a filter and allowed to grow into a continuous epithelial layer. In a mature ALI culture the apical side of the epithelial layer is exposed to air while the basal layer is exposed to growth media positioned beneath the filter. When VA10 cells are cultured in this system they form a pseudostratified epithelial layer. In order to induce pseudostratification the cells are cultured in basal media containing the serum substitute Ultroser G (UG). This composition of growth media promotes cellular differentiation. In turn, these culture conditions results in p63 positive basal cells at the bottom and differentiated p63 negative cells higher in the epithelial layer (Halldorsson et al., 2007).

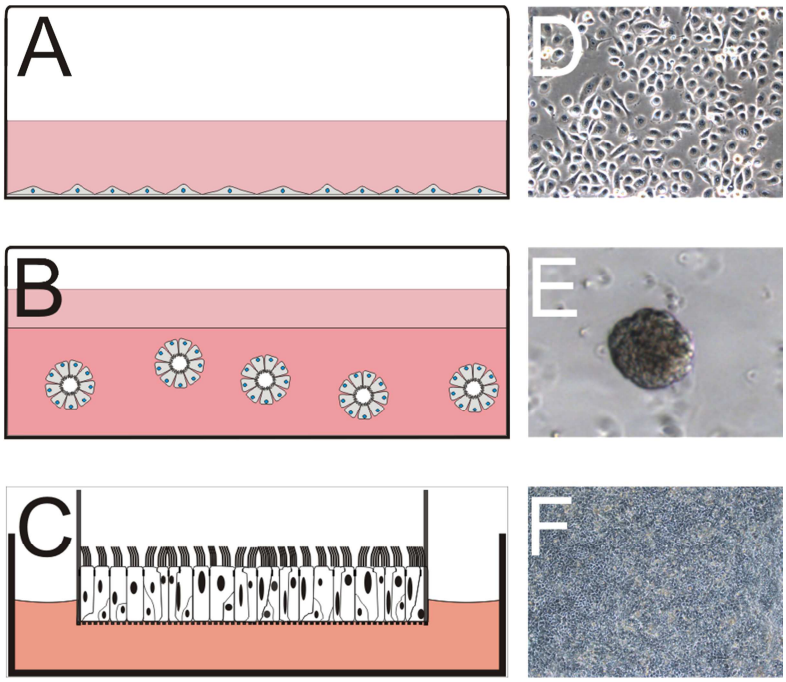

Figure 6: Different culture conditions capture different phenotypic traits. A,D: Traditional monolayer cultures where cells are cultured on a plastic surface. **B,E:** Three-dimensional culture where cells are situated within a reconstituted basement membrane (rBM). These conditions mimic *in vivo* interactions between epithelial cells and the surrounding stromal tissue. **C,F:** Air-liquid interface (ALI) cultures capture the physiological situation of the conducting airways (adapted from (Ingthorsson, 2008).

II – Aim of Study

Human lungs are composed of various types of epithelial cells that reflect their long anatomic distance and their complex function.

Number of diseases affect the lungs, including cancer and lung fibrosis. These are complicated diseases with complex cellular origin. The cellular origin of lung fibrosis is poorly understood. Although, three distinct origins have been suggested for mesenchymal cells involved in fibrosis.

These cells are believed to be either resident lung fibroblasts or myofibroblasts, mesenchymal stem cells from the blood or lung epithelial cells.

The general aim of this project was to explore the plasticity of human lung epithelial cells in terms of their ability to participate in lung fibrosis through process commonly referred to as epithelial-to-mesenchymal transition.

In this project a lung epithelial cell line along with primary lung epithelial cells were cultured both in conventional monolayer cultures as well as more advanced organotypic cultures. Culturing normal human primary lung epithelial cells is a difficult task and in the current literature there is no public consensus regarding the general isolation of these cells or the successful cultivation and isolation of various cell populations. Therefore, much effort was put into refining these protocols during this study. In parallel, a well-defined bronchial epithelial cell line, VA10, was used which was established in the laboratory and has been successfully used in studies on lung stem cell biology.

My experimental objective was to characterize and explore marker expression in fibrotic lung samples *in situ* with emphasis on epithelial-to-mesenchymal transition (EMT). Additionally, I wanted to evaluate the plasticity of lung epithelial cells *in vitro*, also emphasizing their ability to undergo EMT. In order to be able to explore the plasticity of primary lung epithelial cells an isolation protocol for these cells had to be established as well.

Specific objectives:

1) Evaluate marker expression in lung samples from patients suffering from idiopathic pulmonary fibrosis (IPF).
2) Analyze the plasticity of VA10 cells exposed to conditions that favor stem cell and/or mesenchymal differentiation.
3) Establish protocols for culture of human lung epithelial cells.
4) Analyze if primary lung epithelial cells are amenable to mesenchymal transition as tested in objective 2.

III – Materials and Methods

1. Cell culture

All cell cultures were maintained at 37°C and 5% CO_2 concentration.

1.1 Monolayer

1.1.1 VA10

High passage control VA10 cells were maintained on T25 culture flasks (BD Bioscience, USA) in commercially bought LHC-9 bronchial medium (Invitrogen - Gibco) supplemented with 50 U/mL penicillin/streptomycin (Invitrogen - Gibco). Ultroser treated VA10 cells were maintained on commercially bought DMEM (Invitrogen - Gibco) supplemented with 2% Ultroser G (Pall Biosepra, France) and 50U/mL penicillin/streptomycin (Invitrogen - Gibco). Culture media was changed three times a week.

1.1.2 HUVECs

Human Umbilical Vein Endothelial Cells (HUVECs), generously provided by Dr. Haraldur Halldórsson, were maintained on T75 culture flasks (BD Bioscience, USA) in commercially bought EBM-2 (LONZA Group Ltd.) supplemented with human recombinant Epidermal Growth Factor (hEGF), human Fibroblast Growth Factor Basic (hFGF-B), Vascular Endothelial Growth Factor (VEGF), human recombinant Insulin-like Growth Factor (R_3-IGF-1), hydrocortisone, heparin, ascorbic acid (LONZA Group Ltd) and 50 U/mL penicillin streptomycin (Invitrogen - Gibco). In addition, culture media was supplemented with 5% fetal bovine serum (FBS) (Invitrogen - Gibco). Culture media was changed three times a week.

1.2 Three-dimensional culture

For 3D cell cultures, reconstituted basement membrane (rBM, growth factor reduced, Matrigel matrix, BD Bioscience, USA) was used. To induce branching morphogenesis, VA10 cells were co-cultured HUVECs in the ratio 1:100 in 300μL of Matrigel for 24 well plates (Nunc, Thermo Scientific) or 190μL for 48 well plates (Nunc, Thermo Scientific). In other instances, VA10 cells were co-cultured with primary lung fibroblast treated with Mitomycin C (Sigma Aldrich) (10μg/mL) for three hours prior to seeding. Cells were trypsinized and seeded into the Matrigel matrix. The Matrigel was then incubated at 37°C for 30 minutes to induce solidification. The culture was then covered with EGM-2 media (LONZA Group Ltd.) supplemented with 5% FBS (Invitrogen - Gibco) in addition to growth factors previously mentioned (LONZA Group Ltd.) and 50 U/mL penicillin/streptomycin. Culture media was changed three times a week and cultures were usually maintained for 3-4 weeks.

1.3 Primary cell cultures

Detailed isolation protocols for primary lung cells are covered in the *Results* chapter of this thesis. Below is a brief description of culture conditions.

1.3.1 Bronchial cells

Bronchial cells were maintained on collagen coated (Advanced Biomatrix) T25 culture flasks (BD Bioscience, USA) in commercially bought LHC-9 bronchial media (Invitrogen - Gibco) supplemented with 50 U/mL penicillin/streptomycin (Invitrogen - Gibco). Ultroser G (UG) treated bronchial cells were maintained on commercially bought DMEM (Invitrogen - Gibco) supplemented with 2% Ultroser G (Pall Biosepra, France) and 50 U/mL penicillin/streptomycin (Invitrogen - Gibco). Culture media was changed three times a week.

1.3.2 Distal lung cells

Cells isolated from the distal area of the lung were maintained on collagen coated (Advanced Biomatrix) T25 culture flasks (BD Bioscience, USA) in commercially bought DMEM (Invitrogen – Gibco) supplemented with 10% FBS and 50 U/mL penicillin/streptomycin (Invitrogen - Gibco). Culture media was exchanged three times a week.

2. Immunocytochemistry

2.1 Deparaffinization and staining of tissue slides

Paraffin wax was removed by emerging tissue slides in Xylene (J.T Baker) for two rounds of 5 minutes. Slides were then allowed to dry and subsequently submerged in 96% ethanol (Gamla Apótekið), also for two rounds of 5 minutes. Next, the slides were submerged in 70% ethanol for 5 minutes. Slides were subsequently rinsed with running water for 1 minute. Tris-EDTA (TE) buffer (Appendix 1.1) was used for antigen retrieval. The slides were submerged in TE buffer and heated at level 9 for 9 minutes in the microwave. Microwave setting were then changed to level 5 and the slides were incubated for 15 minutes. Slides were allowed to cool for 20 minutes. Next, the slides were rinsed with running water for 10 minutes followed by a 5 minute rinse with PBS.

Prior to staining, slides were blocked for 5 minutes using 10% FBS (Invitrogen - Gibco) in PBS. Next, slides were incubated with primary antibodies (table 2) diluted in 10% FBS for 30 minutes. Slides were then rinsed twice with PBS for 5 minutes. When stained with primary antibodies raised in rabbits the slides were incubated in anti-rabbit secondary antibody (M0737 - DAKO) diluted in 10% FBS for 30 minutes followed by two 5 minute rinse cycles with PBS. Next, the slides were incubated in tertiary antibody (Z056 - DAKO) diluted in 10% FBS for 30 minutes followed by another two 5 minutes PBS rinse cycles. Third, the slides were incubated in quaternary antibody (P850 - DAKO) diluted in 10% FBS for 30 minutes followed by 2x5 minutes PBS rinse. Next, the slides were incubated in activated DAB chromogen (DAKO) for 10 minutes in the hood. Slides were then rinsed with running water, stained with haematoxylin for 30

seconds and viewed in a brightfield microscope (Leica). For slides stained with primary antibodies raised in mice the same protocol was used with the exception of secondary M0737 incubation.

2.2 Staining of monolayer cultures

Cells or cryosectioned lung tissue were either fixed in methanol (Sigma Aldrich) at -20°C for 10 minutes or in 3.5% formaldehyde (Sigma Aldrich) at room temperature for 10 minutes, followed by 0.1% Triton-X (Sigma Aldrich) treatment for 2 x 7 minutes. Unspecific binding was blocked by incubating cells in 10% FBS (Invitrogen - Gibco) in PBS for 5 minutes. Primary antibodies (table 2) were then incubated for 30 minutes diluted in 10% FBS in PBS. For DAB staining, secondary (Z056) and tertiary (P850) antibodies (DAKO) were incubated for 30 minutes each diluted in 10% FBS in PBS. Cells were washed for 2x5 minutes with PBS between and after incubation. Cell nuclei were then stained with haematoxylin for 30 seconds. For IF staining, fluorescent secondary antibodies corresponding to primary antibody isotype (Alexa Fluor, Invitrogen) were incubated for 30 minutes diluted in 10% FBS in PBS and then cell nuclei were stained with ToPro3 (Invitrogen) (1:500) nuclear stain for 15 minutes. For DAB staining signal was detected using an inverted brightfield microscope (Leica). For fluorescent staining a confocal microscope (Zeiss LSM5 Pasqal) was used. Confocal images were processed using Zeiss LSM Image Examiner.

Table 2: List of primary antibodies used for immunostaining in the current study.

Antibody	Clone	Species	Isotype	Dilution*	Fixation	Company
E-cadherin	34	Mouse	IgG2a	1:50/ 1:100	Methanol	BD Bioscience
N-cadherin	32	Mouse	IgG1	1:50/ 1:100	Methanol	BD Bioscience
EpCAM	VU-1D9	Mouse	IgG1	1:50/ 1:100	Methanol	Leica
EpCAM	Polyclonal	Rabbit	IgG	1:25 (DAB)	Formalde-hyde	Abcam
Vimentin	V9	Mouse	IgG1	1:50/ 1:100	Methanol	Dako
Thy1 (CD90)	AS02	Mouse	IgG1	1:50/ 1:100	Methanol	Calbiochem
CK14	LL002	Mouse	IgG3	1:50/ 1:100	Methanol	Abcam
F-actin	Phalloidin	N/A	N/A	1:50/ 1:100	Formalde-hyde	Invitrogen
Fibronectin	LabMab	Mouse	IgG1	1:250 (IF)	Formalde-hyde	N/A

***DAB staining/IF staining**

3. Cell sorting

Cells were sorted using Magnetic Cell Sorting (MACS, Miltenyi Biotec, Germany). Cells were trypsinized and dissolved and spun down at 2000RPM for 3 minutes in commercially bought MACS buffer (Appendix 1.2) (Miltenyi Biotec, Germany). Cells were then incubated, either with primary microbeads for EpCAM (Miltenyi Biotec, Germany) or unconjugated primary antibody (table 3), for 30 minutes at 4°C. Cells were washed by spinning them down at 2000RPM for 3 minutes three consecutive times suspended in MACS buffer. When incubated with primary antibodies, a secondary incubation was conducted using anti-mouse IgG microbeads (Miltenyi Biotec, Germany), for 30 minutes also at 4°C. After incubation cells were washed three times. Cells were then dissolved in 1mL of MACS buffer and either loaded onto manual MACS separation columns (MS or LD columns, Miltenyi Biotec, Germany) or run through an autoMACS cells sorter (Miltenyi Biotec, Germany).

Table 3: List of antibodies used for surface marker cell sorting in the current study.

Antibody	Clone	Species	Dilution*	Company
EpCAM	VU-1D9	Mouse	1:50/1:100	Leica
Thy1	AS02	Mouse	1:50	Calbiochem

***Positive selection/Depletion**

4. Protein extraction

Cultures were washed with ice cold PBS. PBS was then removed thoroughly and replaced with 170µL of RIPA lysis buffer (Appendix 1.3). The culture flask was then left on ice for 10 minutes. Next, cells were scraped from the bottom of the flask using a cell scraper (BD Bioscience, USA). The solution was then placed in a tube and incubated on ice for 10 minutes. The solution was then subsequently centrifuged for 20 minutes at 4°C at 14000 RPM. The supernatant was then collected into a fresh tube and protein concentration measured using the Bradford protein assay.

5. Western blot

For Western blot, 5µg of protein were mixed with 2.5 µL 4X NuPage LDS sample buffer (Invitrogen – Life Technologies) and sterile water (Fresenius kabi) to 9 µL. Samples were then reduced by adding 1µL of Mercaptoethanol (Sigma Aldrich) and heating at 75°C for 10 minutes. Samples were then loaded on 10% SDS Bis-Tris gels (Invitrogen – Life Technologies) and run on 180V for 45 minutes in 1X NuPage MES running buffer (Invitrogen – Life Technologies). Proteins were transferred to a PVDF membrane (Millipore) after methanol (Sigma Aldrich) activation for 30 seconds. Proteins were transferred at 30V for 1.5 hours in 1X NuPage transfer buffer (Invitrogen – Life Technologies) containing 10% methanol.

After transfer, the membrane was washed briefly in PBS at room temperature for 5 minutes and then blocked with 5% BSA (Applichem) or 5% non-fat milk (Mjólkursamsalan) in TBS + 0.1% Tween (Sigma Aldrich) or PBS for 1 hour. Primary antibodies (table 4) were incubated overnight at 4°C in 5% BSA or 5% non-fat milk in 0.1% TBS + Tween. The next day, the membrane was washed for 3x10 minutes in PBS. Secondary infrared (IR) antibodies (LiCOR Biosystems) were incubated in 0.1% TBS-Tween + 0.02% SDS (Sigma Aldrich) for 1 hour at 1:20000 dilution. Subsequently, the membrane was washed for 3x10 minutes in PBS.

Signal detection and analysis were performed using an Oddysey Infrared Image Scanner and the corresponding Image Studio software (LiCOR Biosystems).

Table 4: List of antibodies used for Western blot in the current study.

Antibody	Clone	Species	Dilution	Manufacturer
E-cadherin	34	Mouse	1:2000	BD Bioscience
N-cadherin	32	Mouse	1:2000	BD Bioscience
EpCAM	Polyclonal	Rabbit	1:2000	Abcam
Vimentin	V9	Mouse	1:2000	Dako
Actin	C4	Mouse	1:1000	Abcam

6. Migration assay

20.000 starved cells (24 hours) were seeded onto migration filters (8µm pores, BD Bioscience, USA) in commercially bought DMEM supplemented with 50U/mL penicillin/streptomycin (Invitrogen - Gibco). Endothelial Growth Medium (LONZA Group Ltd.) supplemented with 5% FBS (Invitrogen - Gibco) was then added to the lower well. Cells were allowed to migrate for 24 hours. Cells were then fixed for 5 minutes in 4% formaldehyde (Sigma Aldrich) and then stained with 0.1% Crystal Violet for 15 minutes. Filters were then rinsed with PBS and cells on the apical layer of the filter were wiped off with a Q-tip. Number of migrated cells was determined by counting in three representative areas on each filter using a brightfield microscope (Leica). Each experiment was conducted in triplicate.

7. Soft agar assay

12 well plates (BD Bioscience, USA) were coated with 1% soft agar (Sigma Aldrich) diluted in commercially bought DMEM (Invitrogen - Gibco) and kept at 4°C for 20 minutes to allow solidification. 30.000 cells were then seeded into 0.5% soft agar preheated to 40°C and placed onto the solidified 1% surface. The plate was then incubated at 4°C for 10 minutes to allow solidification of the upper layer. Cells were then cultured for 20 days. After 20 days, cells were stained with 0.005% Crystal Violet for one hour and colonies over 30μm in size were counted in each well using a phase contrast microscope (Leica). Three representative areas were counted in each well. Each experiment was conducted in triplicate.

8. Growth curve

10.000 cells were seeded onto 24 well plates (Nunc, Thermo Scientific) in triplicate. After 24 hours the cells were rinsed with PBS and fixed with 4% formaldehyde (Sigma Aldrich) for 10 minutes at room temperature. The cells were then rinsed with water and stained with 0.1% Crystal Violet for 15 minutes and then subsequently rinsed three times with water. This procedure was repeated for 7 plates over the period of 7 days. The cells were then dissolved in 10% acetic acid (Sigma Aldrich) and 100μL of the solution transferred to a 96 well plate (BD Bioscience, USA) and optical density at 590nm was measured using a spectrometer. OD was then plotted as a function of time, indicating cell growth.

9. RNA isolation

Culture media was aspirated from cultured cells and they incubated in 2mL of TriReagent (Sigma Aldrich) for 5 minutes with gentle pipetting every two minutes. The solution was then transferred to a tube and 0.4mL per mL of TriReagent of chloroform (Sigma Aldrich) was added to each tube. Samples were vortexed for 15 seconds and incubated at room temperature for 15 minutes. Samples were then spun down at 13000RPM for 18 minutes at 4°C. The clear supernatant was then removed and transferred to a new tube. 1mL of isopropanol (Sigma Aldrich) per mL of TriReagent was then added and mixed gently. Samples were incubated at room temperature for 10 minutes and then spun down at 13000RPM for 12 minutes at 4°C. The supernatant was then discarded and the resulting pellet washed in 96% ethanol (Gamla Apótekið). Next, samples were spun down at 8000RPM for 5 minutes. After centrifugation the ethanol was discarded and allowed to evaporate fully from each sample before the RNA pellet was dissolved in RNase free water (Fermentas). RNA concentration and quality was measured using a NanoDrop Spectrometer.

10. cDNA synthesis

Reverse transcription was carried out using the RevertAid First Strand Synthesis Kit (Fermentas). Prior to transcription the isolated RNA was treated with DNase to eliminate genomic DNA contamination. 2µg of RNA were added to an eppendorf tube, along with 2µL of 10X reaction buffer containing $MgCl_2$ (Fermentas) and 2µL (2u) of DNaseI, RNase free (Fermentas, #EN0521). Nuclease free water (Fermentas) was then added to 20µL. Samples were incubated at 37°C for 30 minutes. 2µL of 25mM EDTA (Fermentas) was then added and samples incubated at 65°C for 10 minutes. This prepared RNA was used for the reverse transcriptase reaction.

2µL of random hexamer primers (Fermentas) was added to the prepared RNA, along with nuclease free water. Samples were then mixed gently, centrifuged briefly and incubated at 65°C for 5 minutes. Samples were then subsequently chilled on ice, spun down and kept on ice for the following steps. 4µL of 5X reaction buffer (Fermentas) was added to each sample along with 1µL of RNase inhibitor (Fermentas). 2µL of 10mM dNTP mix (Fermentas) was then added to each tube. Lastly, 1µL of RevertAid H minus M-MuLV Reverse transcriptase (Fermentas) was added. Next, all samples were mixed gently and centrifuged. Samples were then incubated for 5 minutes at 25°C followed by an incubation at 42°C for 60 minutes. Reaction was then terminated by heating the samples at 70°C for 5 minutes. The resulting cDNA product was then used for quantitative real-time PCR (qRT-PCR).

11. qRT-PCR

Each PCR was run with a reaction volume of 10µL using a ROX probe (Fermentas). Three primer mixes were used, primers for GAPDH, miR200c and miR203 (table 5) (Applied Biosystems). Each reaction was carried out in triplicate in addition to a non-template control. Comparative C_T analysis was run for two hours using a traditional TaqMan protocol. Data was analyzed using 7500 Software v2.0 (Applied Biosystems).

Table 5: List of qRT-PCR primers used in the current study.

Gene	Reporter	Quencher	Assay ID
miR200c	FAM	NFQ-MGB	Hs03303157
miR203	FAM	NFQ-MGB	Hs03302931
GAPDH	VIC	NFQ-MGB	4326317E

12. Flow cytometry

Cells were trypsinized and filtered through a 30μm filter (Miltenyi Biotec, Germany). Cells were then blocked in 10% goat serum (Invitrogen - Gibco) for 1 hour at room temperature. After blocking cells were washed with PBS for 3 minutes at 2000 RPM. Cells were then stained with primary antibodies (table 6) for 30 minutes at 4°C. After staining, the cells were washed with PBS for 6 minutes at 1300 RPM. Cells were dissolved in 300μL PBS and analyzed with flow cytometry using MACSQuant (Miltenyi Biotec, Germany).

Table 6: Overview of antibodies used for flow cytometry in the current study.

Antibody	Species	Isotype	Conjugation	Dilution	Manufacturer
CD24	Mouse	IgG2a	PE	1:100	BD Bioscience
CD44	Rat	IgG2b	FITC	1:100	BD Bioscience
EpCAM	Mouse	IgG1	APC	1:200	Miltenyi Biotec
Thy1	Mouse	IgG1	PE	1:100	BD Bioscience

13. Apoptosis assay

Cells were treated with the apoptosis inducing drug Camptothecin (CPT - 10 μM) (Sigma Aldrich) for 4 hours at 37°C at 5% CO_2 concentration. Cells were then trypsinized and dissolved in 1X Annexin V binding buffer (BD Bioscience, Apoptosis Detection Kit II) and stained with Annexin V and Propidium Iodine (BD Bioscience, Apoptosis Detection Kit II) for 15 minutes at room temperature in the dark. Cells were washed in binding buffer at 1300 RPM for 6 minutes. Cells were then analyzed by flow cytometry using MACSQuant (Miltenyi Biotec, Germany).

14. Statistical analysis

Data is presented as mean and standard deviation (error bars) from number of independent experiments. Graphs and calculations were done using GraphPad Prism or Microsoft Excel.

Two-tailed student's T-test was performed using GraphPad Prism. P values lower than 0.05 were considered statistically significant.

IV – Results

1. Histological overview of lung epithelial and mesenchymal compartments

Due to the complexity and size of the human lung its histology is quite intricate. In order to be able to put my work with lung epithelial cells *in vitro* in context with the *in situ* environment of the lungs it is imperative to be familiar with the distribution of both epithelial and mesenchymal cells in lung tissue.

1.1 Normal lung tissue

In order to gain overview over the cellular context of lung epithelium and the surrounding mesenchyme the expression of common epithelial and mesenchymal markers was assessed by staining normal human lung samples. Lung epithelium is highly positive for EpCAM, a general epithelial marker (figure 7 left, upper panel) while it exhibits a moderate expression of E-cadherin (figure 7 middle, upper panel, arrows). In the epithelium, few CK14 positive cells can be seen (figure 7 right, upper panel, arrows). These CK14 positive cells are believed to be the basal cells responsible for replenishing the bronchial epithelium. The mesenchymal markers Vimentin, N-cadherin and Thy1 are, as to be expected, predominantly expressed in the mesenchymal compartment (figure 7, lower panel). Additionally, few Vimentin positive cells can be observed in the epithelium (figure 7 left, lower panel, arrows).

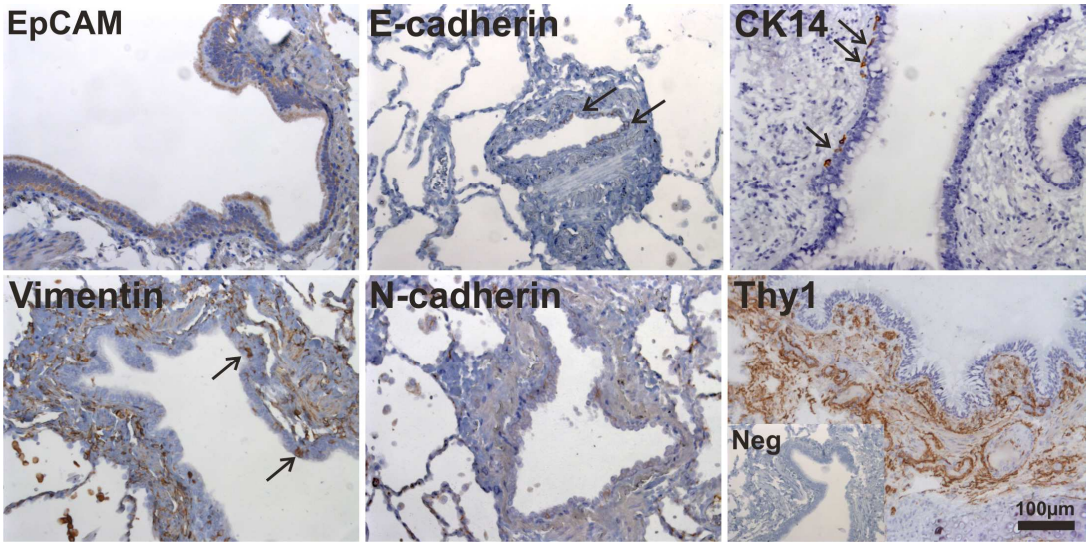

Figure 7: Distinct expression of epithelial and mesenchymal markers in human lung tissue. EpCAM is strongly expressed in lung epithelium. Subtle E-cadherin expression is also observed in the epithelial layer (middle upper panel, arrows) while only a few basal epithelial cells are positive for CK14 (right upper panel, arrows). Vimentin and N-cadherin are almost exclusively expressed in the surrounding msenchyme/stroma. Although, few Vimentin positive epithelial cells are present (left lower panel, arrows). Thy1 predominantly stains mesenchymal cells in the stroma (right lower panel). This work was done in collaboration with Department of pathology at Landspítali and Ari Jón Arason.

1.2 Fibrotic lung tissue

The histology of idiopathic pulmonary fibrosis (IPF) differs substantially from the histology of the normal lung. The characteristic features of IPF are so called fibroblastic foci that are found within the lung tissue. These foci are composed of fibroblast and myofibroblasts and will eventually cause a loss of function in the surrounding lung epithelium. When samples collected from patients with IPF are stained with CK14 and Vimentin one can see a clear increase in the number of positive epithelial cells (figure 8, lower panel) when compared to normal samples (figure 8, upper panel). Additionally, these cells can now be observed throughout the entire fibrosis adjacent epithelium. Under normal conditions CK14 is only expressed in few basal epithelial cells and Vimentin is strongly expressed in the surrounding mesenchyme although a few Vimentin positive cells can be seen distributed randomly throughout the epithelium (upper panel, arrows).

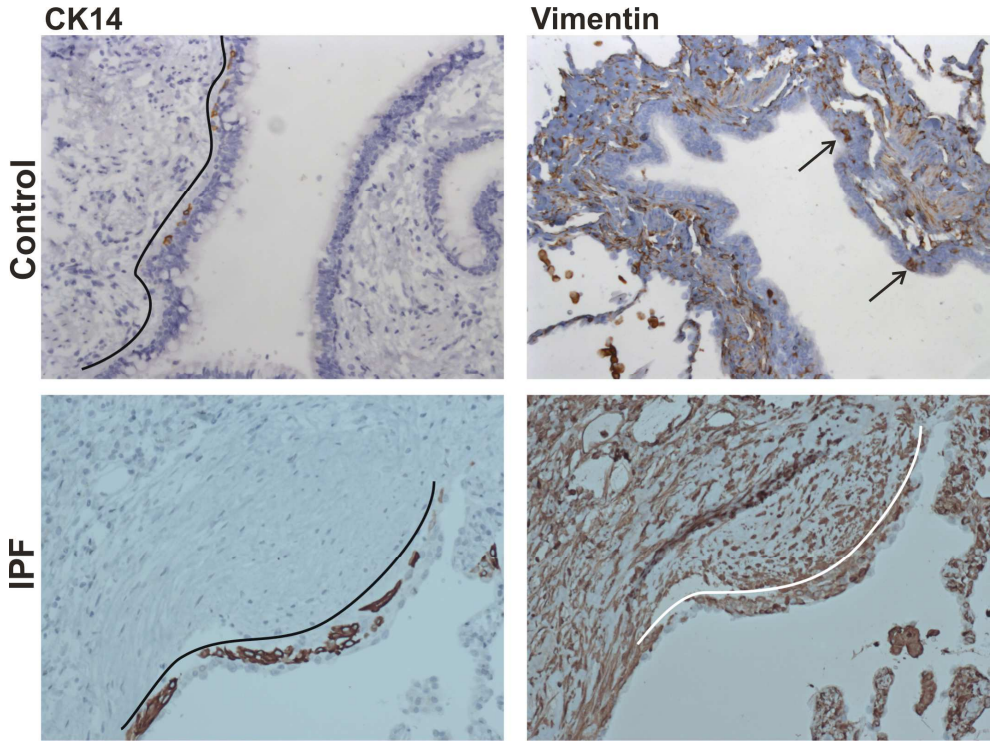

Figure 8: Epithelium associated with IPF histology is enriched for CK14 and Vimentin expressing cells. When samples from IPF patients (lower panel) are compared to control samples (upper panel) a clear increase in CK14 and Vimentin positive cells is observed in fibrosis adjacent epithelium (lower panel, below line). Additionally, CK14 expression seems to be distributed throughout the entire epithelium instead of being expressed only in few basal cells. Vimentin is highly expressed throughout the epithelium in IPF samples. This work was done in collaboration with Department of pathology at Landspítali and Ragnar Pálsson.

The expression of CK14 and Vimentin around fibroblastic foci in IPF indicates the presence of reactive pulmonary epithelium with increased plasticity towards a mesenchymal phenotype. In order to evaluate whether lung epithelial cells in culture could capture phenotypic traits observed in IPF patients I confronted VA10 cells with culture conditions that facilitate differentiation. Initially, however, basic characterization of VA10 cells in culture was conducted.

1.3 VA10

VA10 cells exhibit a cobblestone shape and a basal cell expression profile (Halldorsson et al., 2007). In most cells. there is a relatively homogenous expression of E-cadherin and CK14. Additionally, many cells are also positive for EpCAM. The cells are negative for Thy1 (CD90), a fibroblast marker, which is consistent with their epithelial phenotype. Additionally, little expression of the mesenchymal marker N-cadherin is observed in these cells. Interestingly, unlike *in vivo* lung epithelium where only sporadic Vimentin positivity is observed, most VA10 cells are also positive for Vimentin (figure 9). Traditionally, Vimentin is only expressed in mesenchymal cells (Eriksson et al., 2009). It should, however, be mentioned that Vimentin expression is commonly found in cultured epithelial cells from various organs. It is believed that Vimentin is upregulated when the cells are removed from their three-dimensional context and gain increased growth rate in cell culture (Dairkee et al., 1985; Mark et al., 1990). Therefore, the Vimentin expression in VA10 does not directly indicate that the cells have mesenchymal characteristics but rather indicates a cell culture artifact since VA10 exhibits an otherwise strong epithelial expression profile.

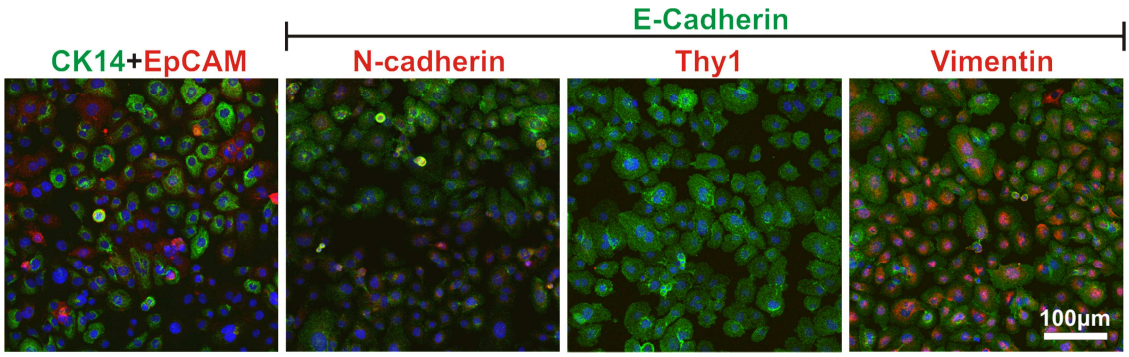

Figure 9: VA10 cells uniformly express E-cadherin and Vimentin. VA10 cells are highly positive for CK14, E-cadherin and Vimentin. EpCAM expression is also observed in a large number of cells. Very little expression of N-cadherin is observed while the cells are completely negative for the fibroblast marker Thy1. Bar 100µm.

2. VA10 cells can generate mesenchymal-like cells in culture

When VA10 cells are cultured in basal media (DMEM) containing the serum substitute Ultroser G (UG) a subset of cells undergoes distinct morphological changes. They lose their cobblestone appearance and become elongated (figure 10A, arrows). In addition they lose their epithelial marker expression and gain a mesenchymal-like expression profile (figure 10, B and C). The mesenchymal subgroup is EpCAM and E-cadherin negative while being N-cadherin positive (figure 10B, arrows and 10C, outline).

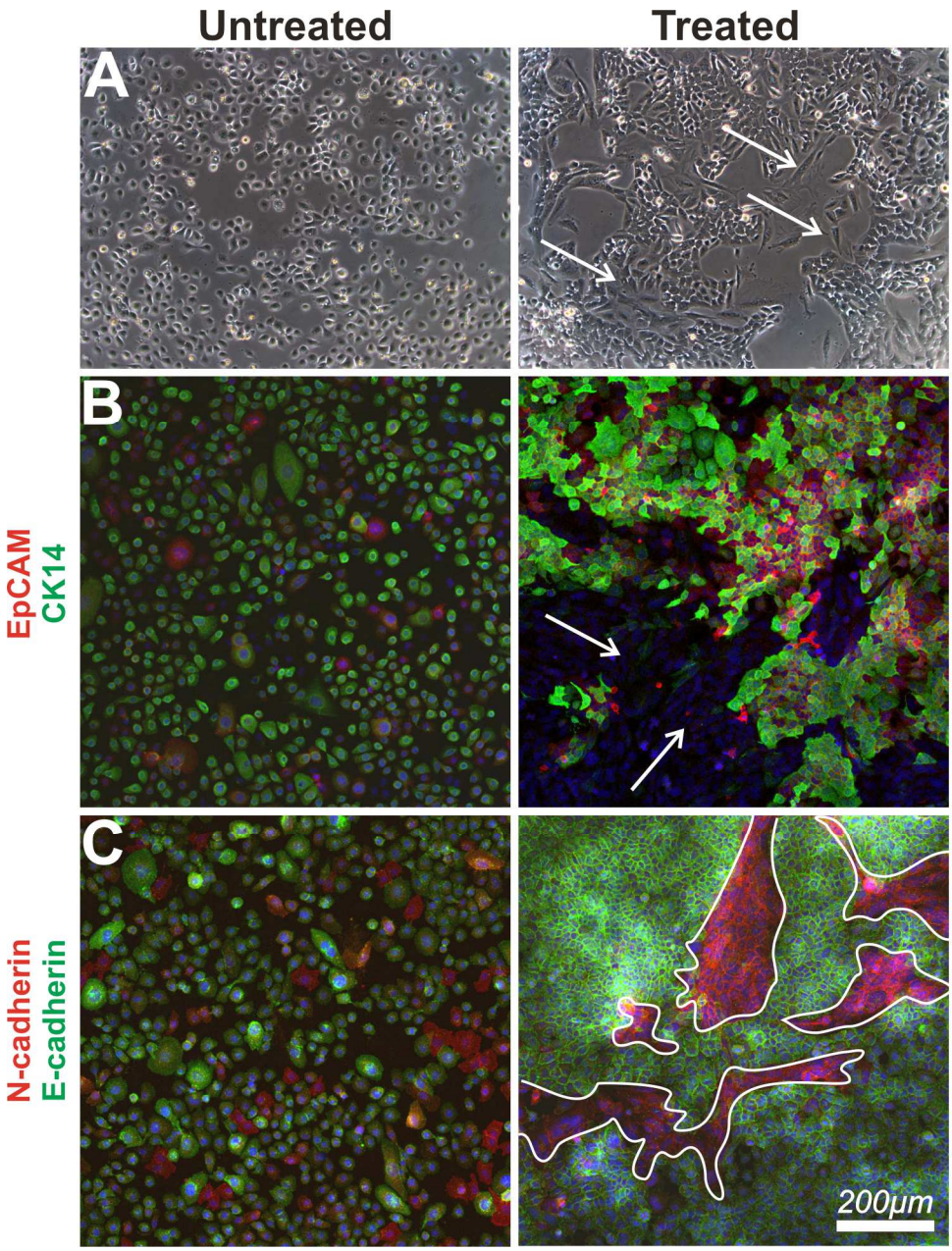

Figure 10: VA10 cells treated with Ultroser G generate mesenchymal-like cells in culture. A: Elongated mesenchymal-like cells are clearly visible in phase contrast images. **B:** Immunostaining reveals an EpCAM negative mesenchymal subgroup (arrows). **C:** This same subgroup is N-cadherin positive (outline). Bar 200µm.

3. Characterization of selective subgroups of VA10

3.1 Mesenchymal like subgroup within UG-treated VA10 cells is EpCAM negative

Since the mesenchymal like subgroup within UG-treated VA10 cells has no noticeable EpCAM expression compared to the epithelial subgroup (figure 10B, arrows), the two cellular subgroups were separated with magnetic cell sorting (MACS) according to their EpCAM expression status and the resulting cellular sublines designated VA10 EpCAM^{low} and VA10 EpCAM^{high}, respectively.

This isolation method returned a stable subgroup of VA10 cells expressing epithelial markers (VA10 EpCAM^{high}) (figure 11A, left and B, upper panel). However, the column flow through (expected to be EpCAM negative cells) still contained few cells with high EpCAM expression (figure 10A,right, arrows). Despite this impurity, the two isolated subgroups have a different overall phenotype and vary substantially in size and morphology, the mesenchymal cells being larger and more spindle shaped.

Expressional differences between the two isolated sublines are also quite distinct. EpCAM^{high} cells are tightly packed and therefore exhibit a high expression of the epithelial cell adhesion molecules EpCAM and E-cadherin. Additionally, Vimentin expression in those cells is severely reduced (figure 11B, upper panel). Additionally, these cells do not express the mesenchymal markers fibronectin, N-cadherin or Thy1 (figure 11A left and 11B, upper panel). The EpCAM^{low} cells, however, exhibit an increase in the expression of mesenchymal markers. Vimentin is strongly expressed along with N-cadherin and Thy1 (figure 11B, lower panel). Additionally, the mesenchymal-like subgroup is positive for fibronectin (figure 10A, right). As previously mentioned, epithelial cells can still be found within this subline. E-cadherin, EpCAM and CK14 positive cells are still visible in these cultures (figure 11B, lower panel, arrows).

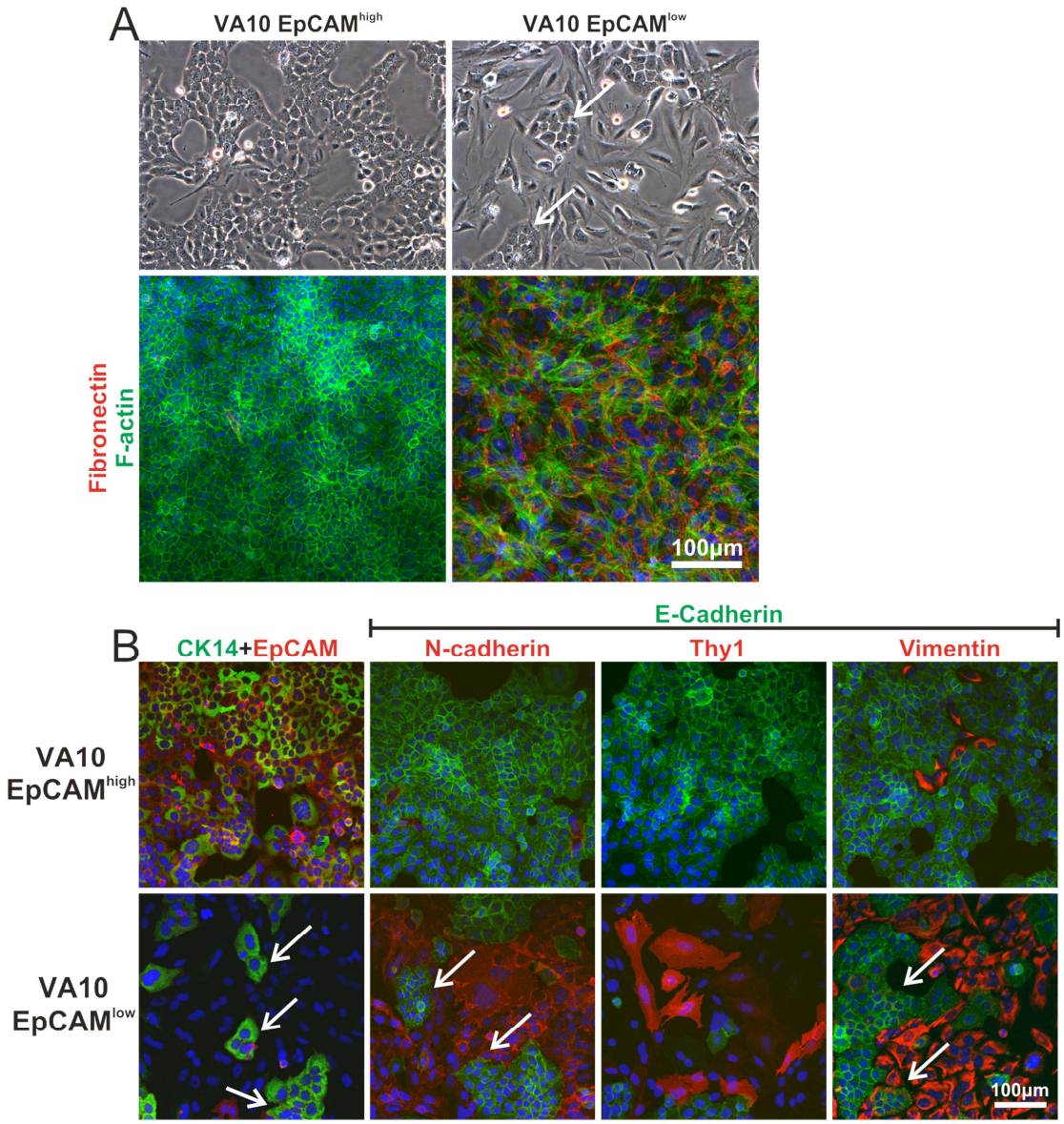

Figure 11: EpCAM high and low expressing subgroups exhibit a difference in phenotype and marker expression. A: EpCAM high expressing cells have a cobblestone appearance while EpCAM low expressing cells are more elongated. VA10 EpCAM^{low} cells are fibronectin positive. **B:** EpCAM low expressing cells have increased expression of Thy1, N-cadherin and Vimentin while EpCAM high expressing cells are positive for E-cadherin and CK14. E-cadherin positive cells are still visible in the EpCAM low expressing subline (lower panel, arrows).

3.2 Thy1 sorting gives rise to a pure mesenchymal-like subgroup

In order to produce a true mesenchymal population free of E-cadherin positive epithelial cells, EpCAM low expressing cells were further sorted for Thy1 (CD90), an anti-fibroblast marker. The resulting subline, designated VA10 Thy1^{pos}, is void of cells with epithelial characteristics (figure 12A, right) containing only cells positive for N-cadherin, Thy1 and Vimentin while being EpCAM and E-cadherin negative (figure 12B, lower panel). However, a few elongated CK14 positive cells are still observed (figure 12B, lower panel, circle). Western blot analysis confirms the down-regulation of epithelial markers in Thy1^{pos} cells (figure 12C).

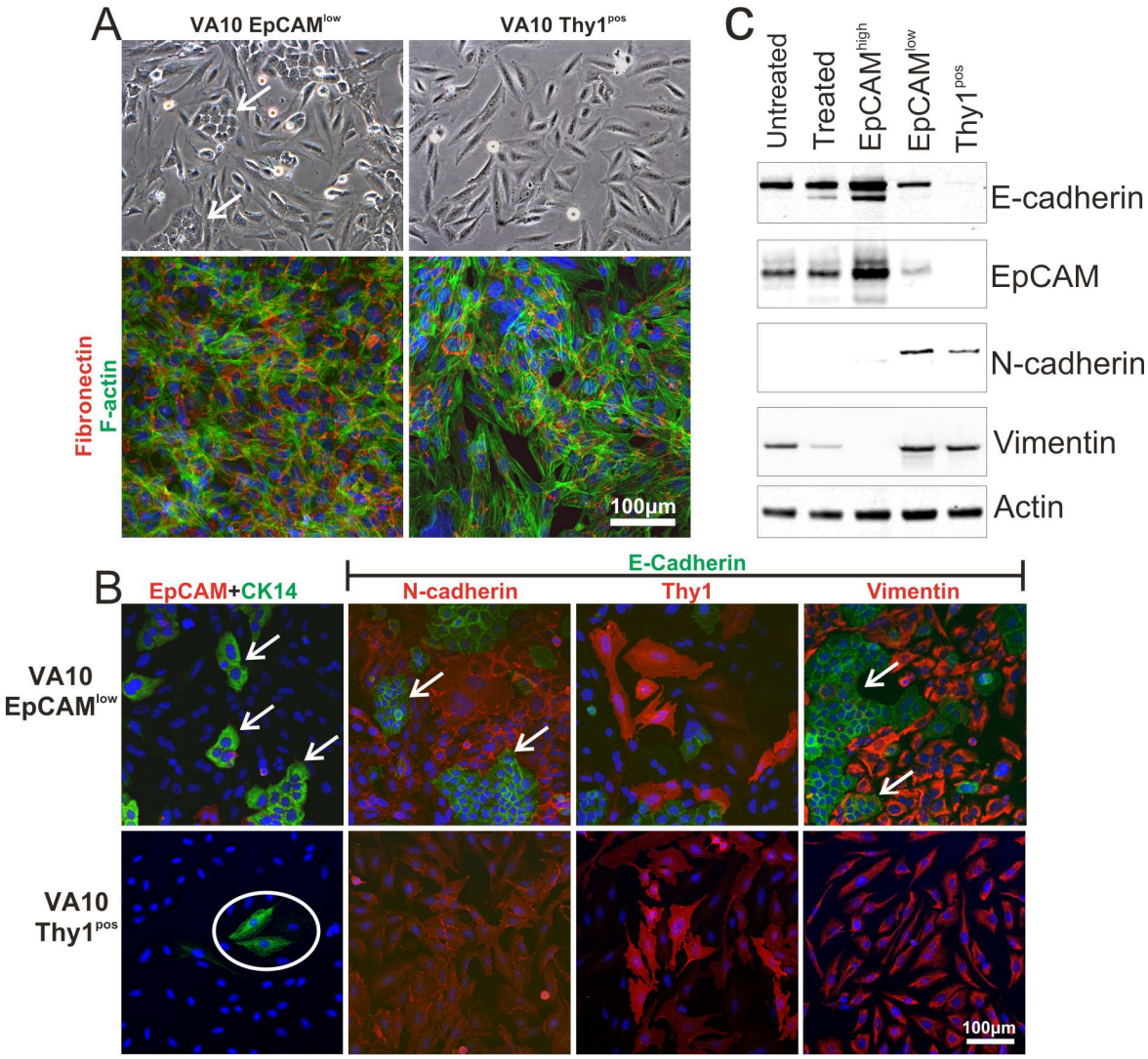

Figure 12: Thy1 sorted cells have a characteristic mesenchymal-like phenotype and marker expression void of all epithelial cells. A: After Thy1 sorting no epithelial like cells are present in the Thy1 positive subline when viewed with phase contrast microscopy. EpCAM^{low} and Thy1^{pos} cells share a similar fibronectin expression in monolayer culture. **B:** The mesenchymal markers N-cadherin, Thy1 and Vimentin become dominant in Thy1 sorted VA10 cells. No EpCAM or E-cadherin expression is observed in these cells and the expression of CK14 is severely reduced (lower panel, circle). Bar 100µm. **C:** Western blot analysis demonstrates down-regulation of epithelial markers in the mesenchymal-like VA10 cells. In these same cells mesenchymal marker expression is increased.

Flow cytometry analysis of both VA10 and its isolated sublines reveals an expressional change in UG-treated cells. The EpCAM high expressing subline exhibits low expression of both CD24 and CD44. The isolated mesenchymal cells, however, exhibit high expression of CD44 while exhibiting low expression of CD24 (figure 13). The $CD44^{high}/CD24^{low}$ phenotype has previously been denoted as a malignant mesenchymal breast cancer stem cell phenotype. It was found that this phenotype could be induced in epithelial cells with EMT inducing agents (Blick et al., 2010; Radisky & LaBarge, 2008; V. Sigurdsson et al., 2011). Interestingly, the Thy1 sorted cells do not seem to be completely negative for EpCAM when analyzed with flow cytometry (figure 13).

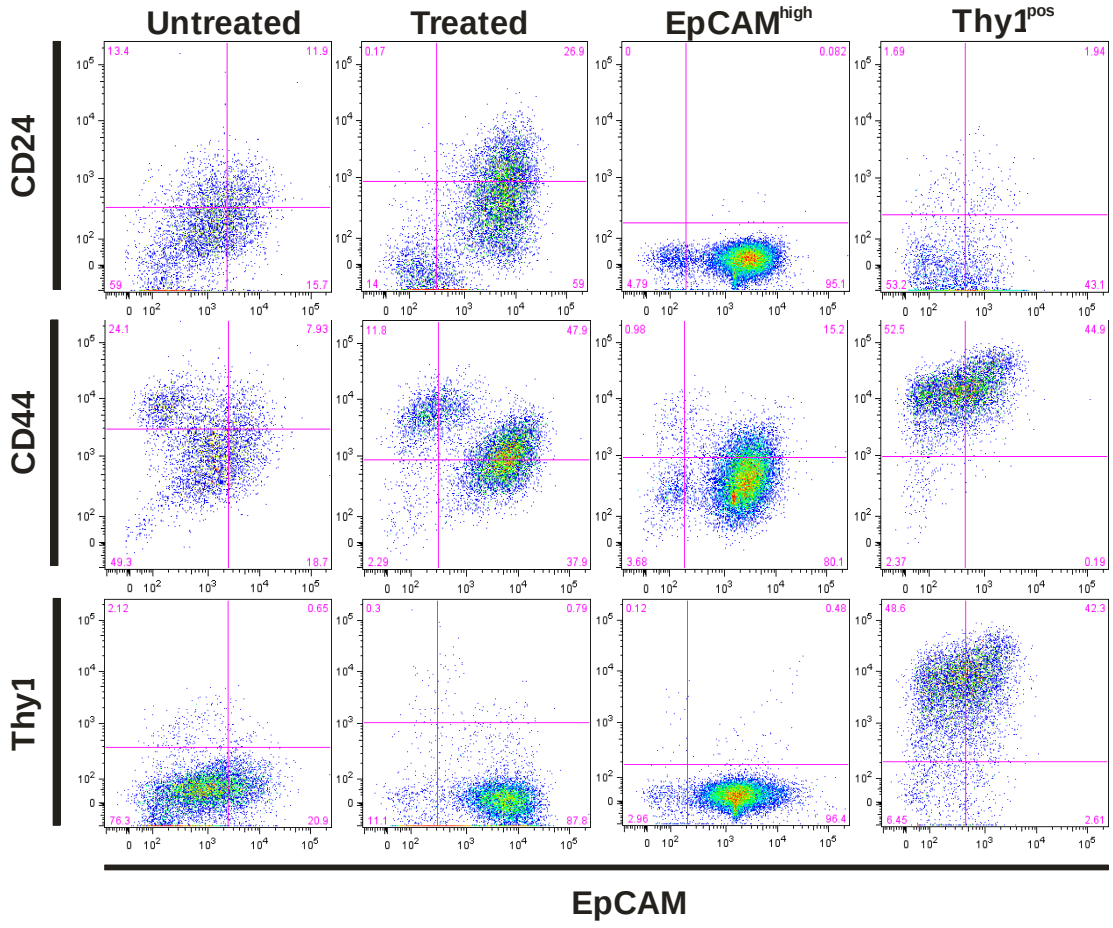

Figure 13: Flow cytometry analysis of VA10 and its sublines demonstrates an expressional difference between treated and untreated cells as well as the isolated sublines. Analysis reveals two distinct subgroups in treated VA10 cells. Additionally it demonstrates the differences between the isolated sublines when it comes to the expression of CD24, CD44, EpCAM and Thy1. EpCAM high expressing cells are $CD24^{low}/CD44^{low}$ while the $Thy1^{pos}$ mesenchymal subgroup exhibits a malignant $CD24^{low}/CD44^{high}$ phenotype.

3.3 UG-treated VA10 cells grow to a higher density than original VA10 cells

When growth density is measured, UG-treated VA10 cells exhibit the fastest growth determined by the measurement of optical density (OD) (figure 14). In this assay, VA10 Thy1^{pos} cells exhibit the lowest density even if they grow equally as fast as treated VA10 cells when observed in culture. Due to the difference in their morphology and size compared to the other cell lines it is not surprising that fewer Thy1^{pos} cells are observed in a density dependent assay. Additionally, it is not uncommon for mesenchymal cell to maintain their individuality in culture and not form a continuous cell layer like epithelial cells.

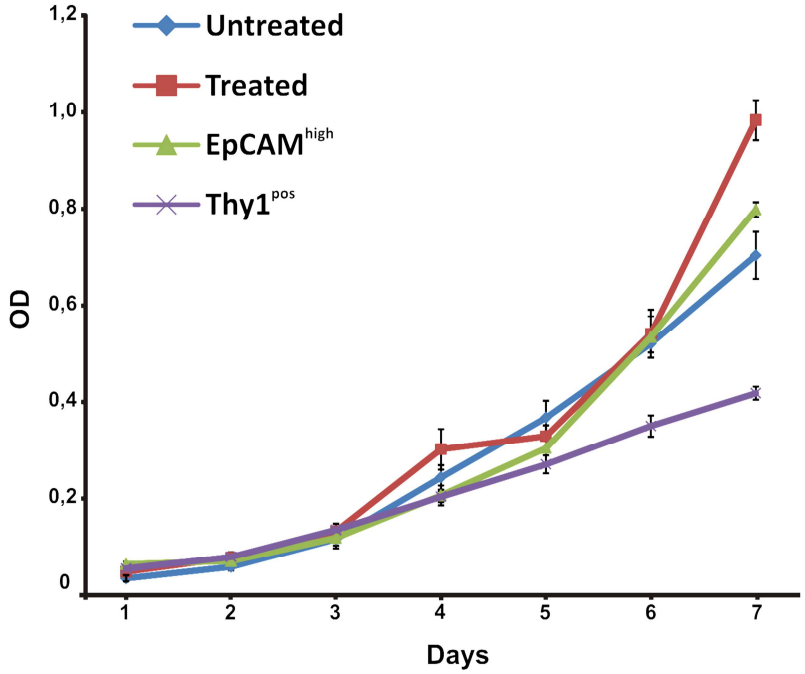

Figure 14: Treated VA10 cells grow to a higher density than original VA10 cells. Both treated and EpCAM high expressing cells grow to a higher density than untreated VA10 cells and VA10 Thy1^{pos} cells. However, when observed in culture VA10 Thy1^{pos} cells grow equally fast as the other treated cells but never grow to a high density.

3.4 VA10 Thy1^{pos} cells can no longer undergo branching morphogenesis

When cultured in 3D co-cultures with endothelial cells, both treated VA10 cells and VA10 EpCAM^{high} form branching bronchioalveolar-like structures like the original VA10 cell line as previously described (Franzdottir et al., 2010). However, when VA10 Thy1^{pos} cells are cultured in the same three-dimensional co-culture system they do not exhibit any branching morphogenesis but still form relatively small solid round colonies (data not shown).

In order to determine which subgroup is responsible for the formation of bronchioalveolar-like structures in treated VA10 cells GFP expressing VA10 EpCAM^{high} and Thy1^{pos} cells were generated. Next, VA10 EpCAM^{high} – GFP cells were mixed with non-GFP expressing VA10 Thy1^{pos} and vice versa. These mixtures were then seeded into 3D co-cultures with endothelial cells. When the resulting structures were analyzed, it turned out that only EpCAM^{high} cells were able to form bronchioalveolar-like structures. In EpCAM^{high} – GFP and Thy1^{pos} mixed cultures all resulting structures were GFP positive (figure 15A). However, when the opposite mixture of cells was investigated all resulting structures were GFP negative (figure 15B). This indicates that the mesenchymal cells cannot form bronchioalveolar-like structures in 3D co-cultures. Although, they did form GFP positive disintegrated spindle colonies characteristic of cells that have undergone EMT (figure 15B, arrows) (V. Sigurdsson et al., 2011).

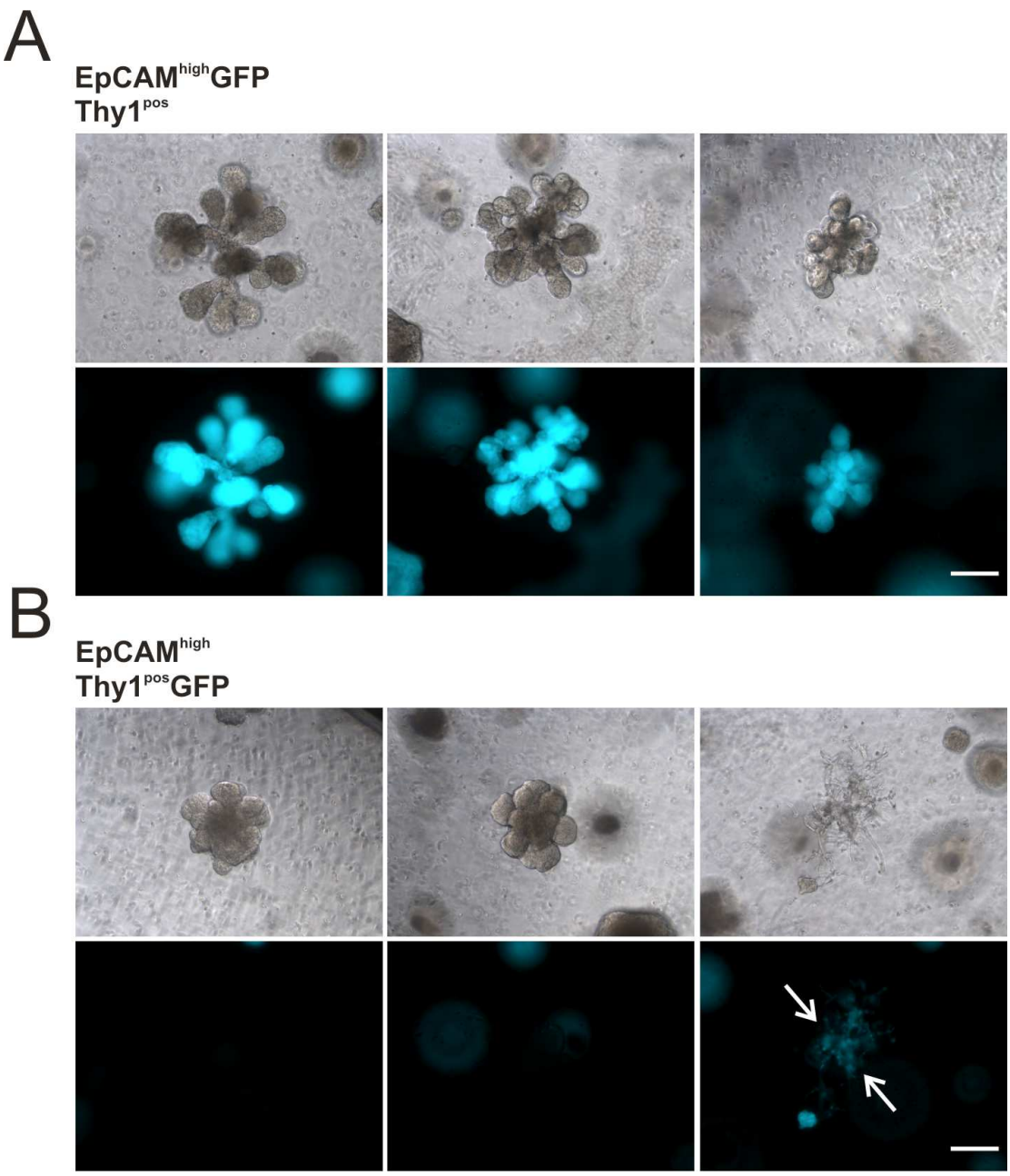

Figure 15: VA10Thy1^{pos} cells do not form bronchioalveolar-like structures in 3D co-cultures. A: All bronchioalveolar-like structures in EpCAM^{high} –GFP and Thy1^{pos} mixed cultures are GFP positive. **B:** Thy1 positive cells have lost their potential to form branching colonies. No bronchioalveolar-like structures are GFP expressing when Thy1^{pos} –GFP cells are seeded into 3D co-cultures. In contrast, they have gained the potential to form spindle colonies (arrows). Bar 200μm.

The percentage of branching colonies in untreated and UG-treated VA10 cells along with the isolated epithelial subline is around 8-12% (figure 16 and (Franzdottir et al., 2010)) In EpCAM^{low} cells it has decreased to around 2% and for Thy1^{pos} cells the percentage of branching cells is zero. Spindle colonies do, however, account for about 10% of their total colony number (figure 16, grey column).

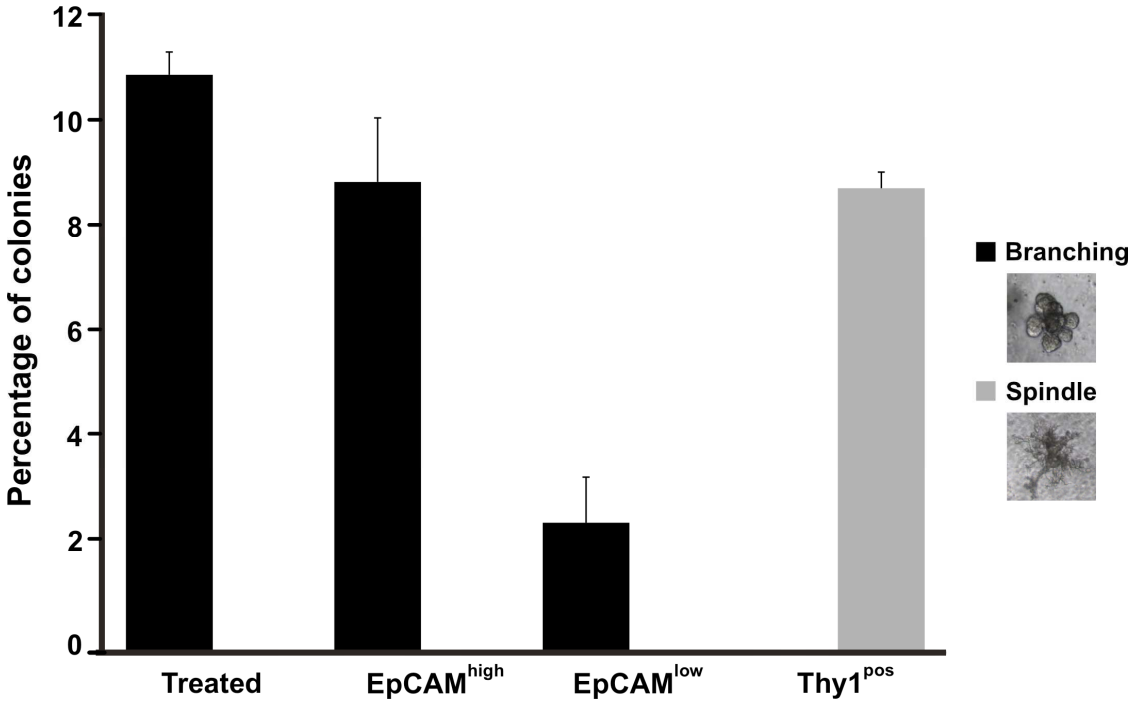

Figure 16: Thy1 positive cells form spindle colonies in 3D co-cultures. Treated VA10 cells along with EpCAM^{high} cells exhibit similar branching percentage as untreated VA10 cells. EpCAM^{low} have a severely diminished branching capacity while Thy1^{pos} cells do not form branching structures at all. In contrast, Thy1^{pos} cells have gained the potential to form spindle colonies in 3D gel cultures.

3.5 VA10 Thy1^{pos} cells exhibit increased anchorage independent growth and migration

Major characteristic of a mesenchymal phenotype is increased ability for anchorage independent growth along with increased migratory potential.

When VA10 Thy1^{pos} cells are grown in soft agar they show an increase in growth compared to the original VA10 cell line, which does not grow in soft agar (Halldorsson et al., 2007) and its epithelial counterpart VA10 EpCAM^{high} (figure 17).

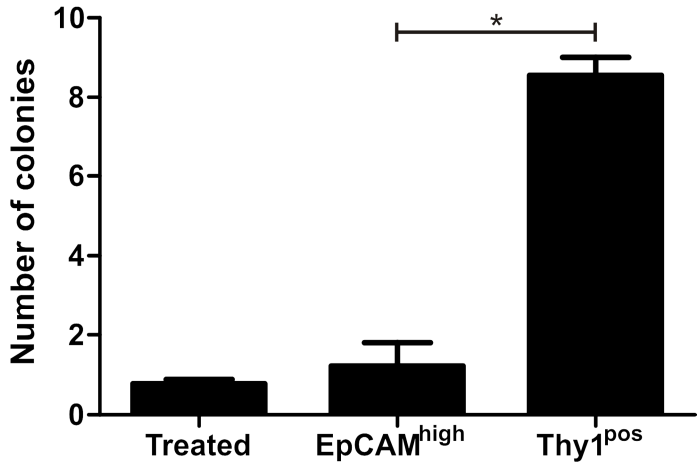

Figure 17: VA10 Thy1^{pos} cells exhibit increased anchorage independent growth. When cultured in soft agar Thy1^{pos} cells show a higher potential for anchorage independent growth than both treated VA10 cells and EpCAM^{high} cells. Colonies larger than 30μm were counted. Each experiment was conducted in triplicate. *P-value 0.0006.

VA10 Thy1^{pos} cells also exhibit increased migration compared to VA10 EpCAM^{high} cells (figure 18). This is consistent with their mesenchymal phenotype.

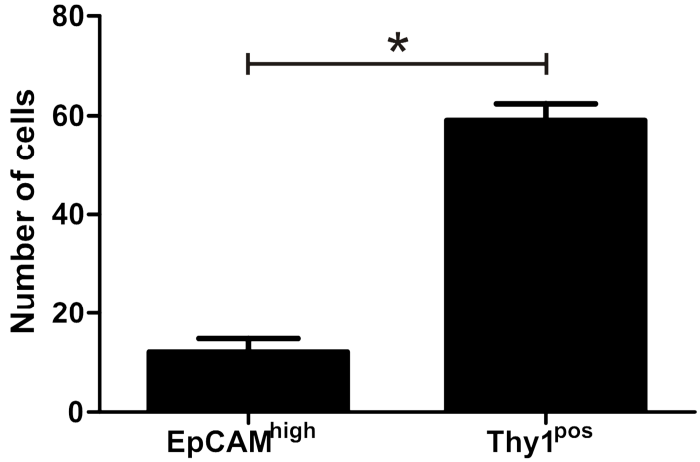

Figure 18: Thy1 positive cells have increased migratory potential compared to EpCAM high expressing cells. Thy1^{pos} cells migrate more actively than EpCAM^{high} cells after 24 hours of starvation. Cells in three representative areas of each migration filter were counted. Each experiment was conducted in triplicate. *P-value 0.0004.

3.6 MicroRNA 200c is downregulated in VA10 Thy1^{pos} cells

Quantitative real time PCR analysis showed that both treated and untreated VA10 cells along with the isolated epithelial subline express microRNA 200c while there is virtually no observed expression in VA10 Thy1^{pos} cells (figure 19A). This expressional difference is consistent with epithelial-to-mesenchymal transition where downregulation of miR200c causes transcriptional repression of E-cadherin via ZEB1 and ZEB2 transcription factors (Gregory et al., 2008).

Additionally, microRNA 203 is highly upregulated in EpCAM^{high} cells while very little expression is observed in Thy1^{pos} cells. Interestingly, the same low expression is observed in the original VA10 cell line as well as unsorted VA10 UG cells (figure 19B). MicroRNA 203 has been reported to be upregulated in primary breast tumors and non-metastatic breast cancer cell lines while hypermethylation of its promoter results in down-regulation during metastatic conditions (Zhang et al., 2011).

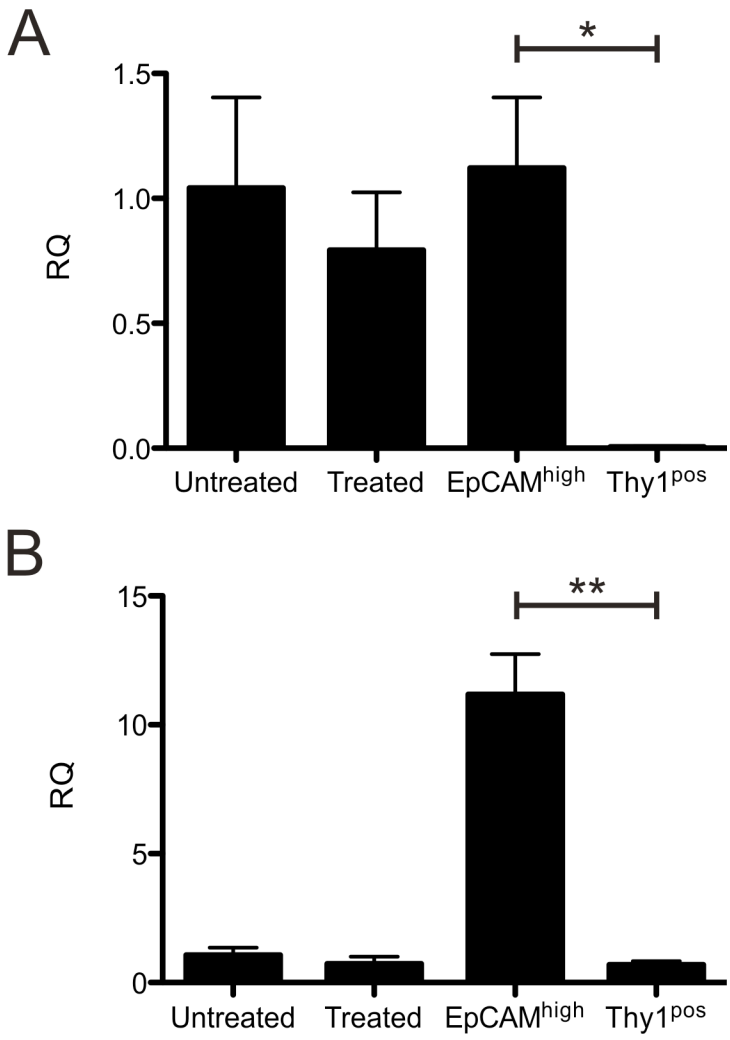

Figure 19: microRNA expression in isolated sublines is consistent with EMT. qRT-PCR analysis of microRNAs 200c and 203 revealed an expressional difference, *P-value 0.0203. **A:** microRNA200c is down regulated in VA10 Thy1 positive cells. **B:** microRNA203 is upregulated in VA10 EpCAM^{high} cells, **P-value 0.0026.

3.7 VA10 Thy1^{pos} cells exhibit increased resistance to apoptosis induction

One of the hallmarks of cancer stem cells and cells that have undergone EMT is acquired resistance to apoptosis.

When the isolated sublines, VA10 EpCAM^{high} and VA10 Thy1^{pos}, are treated with the cytotoxic topoisomerase I inhibitor camptothecin (CPT) and analyzed by flow cytometry Thy1^{pos} cells exhibits an increased resistance to apoptosis induced by CPT. The baseline apoptosis percentage for both sublines is around 11%. After induction around 43% of EpCAM^{high} cells test positive for apoptosis while only 15% of Thy1^{pos} cells do (figure 20). Apoptotic cells are considered to be both Annexin V and PI positive as Annexin V stains cells in early apoptosis while Propidium Iodine (PI) stains cells that have progressed to the later stages of cell death.

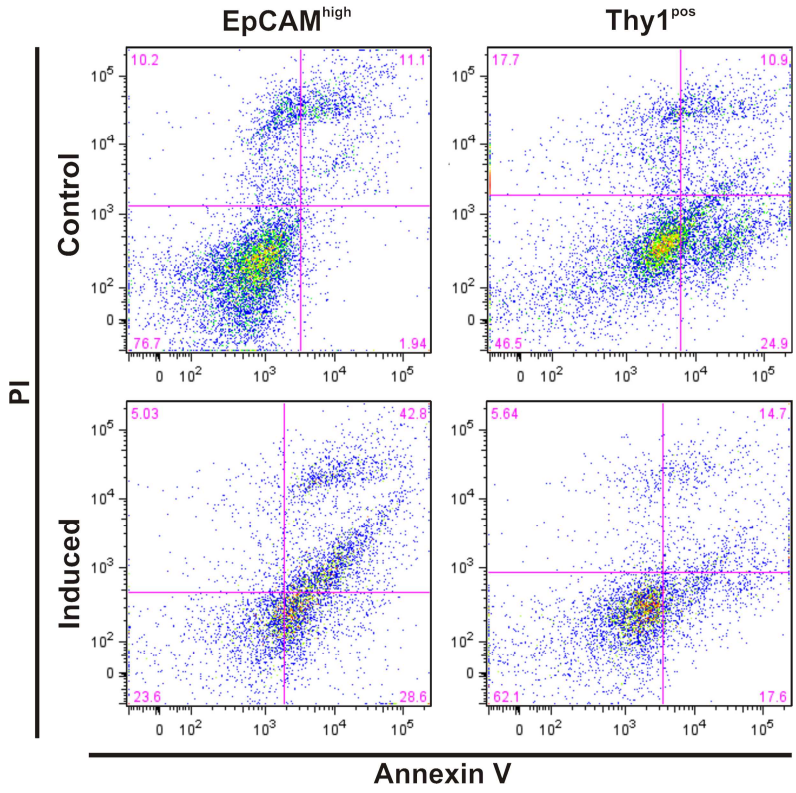

Figure 20: Thy1^{pos} cells have increased resistance to CPT induced apoptosis. The percentage of apoptotic EpCAM^{high} cells (Annexin V^{pos} / PI^{pos}) increases substantially after CPT induction while the percentage of apoptotic Thy1^{pos} cells largely remains the same.

4. Ultroser G induced EMT in VA10 is partially reversible

Mesenchymal-like VA10 Thy1^{pos} cells are capable of partially reverting back to original VA10 phenotype when re-cultured on traditional bronchial medium (LHC-9) (figure 21, reverted). When these reverted cells are then re-treated with Ultroser G they are capable of generating both epithelial and mesenchymal subgroups (figure 21, re-treated, outline). Their marker expression profile moves from a true mesenchymal profile (figure 12B, lower panel) to being mixed where both N-cadherin and E-cadherin positive cells are present in culture (figure 21, re-treated).

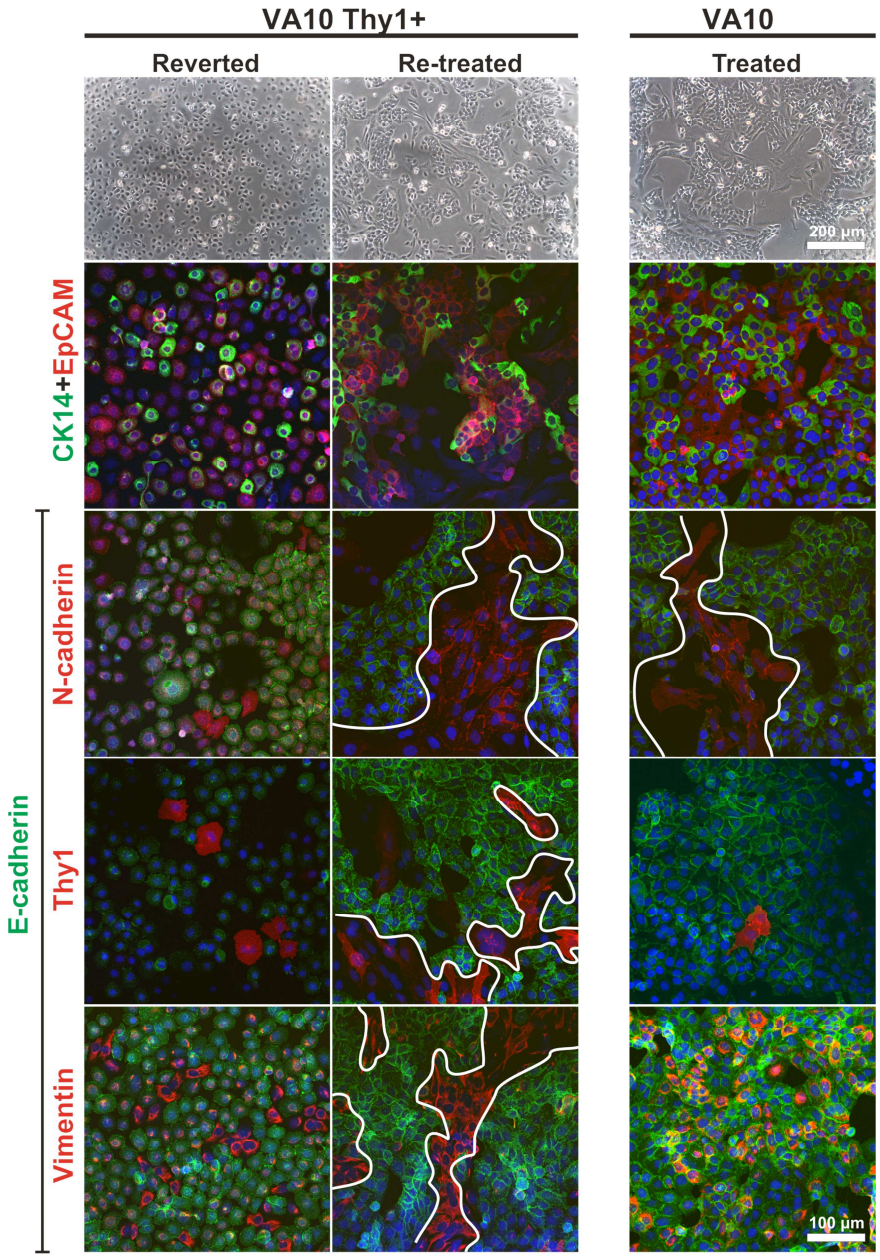

Figure 21: Thy1 positive cells can partially revert back to original epithelial phenotype. Thy1^{pos} cells are capable of reverting back to epithelial phenotype when cultured on traditional bronchial medium (reverted). When re-treated with media containing Ultroser G two distinct phenotypes can be seen, EpCAM, CK14 and E-cadherin positive epithelial cells versus N-cadherin, Thy1 and Vimentin positive mesenchymal-like cells (re-treated, outline). Bars 200 and 100µm.

5. Establishment of primary cell cultures

As previously mentioned, the establishment of primary cultures is extremely important to correctly capture *in vivo* conditions and supplement experimental data acquired using immortalized cell lines.

5.1 Cell isolation

Many different laboratories have been isolating lung epithelial cells from fresh human lung tissue (Daum et al., 2012; Fujino et al., 2011). Cell isolation from primary lung tissue is known to be difficult. The histological complexity of the human lung requires distinct isolation protocols for the different anatomical regions. So far, cells have been isolated from bronchial epithelium as well as from the alveolar regions. The isolation protocols for these two distinct regions differ substantially (figure 22).

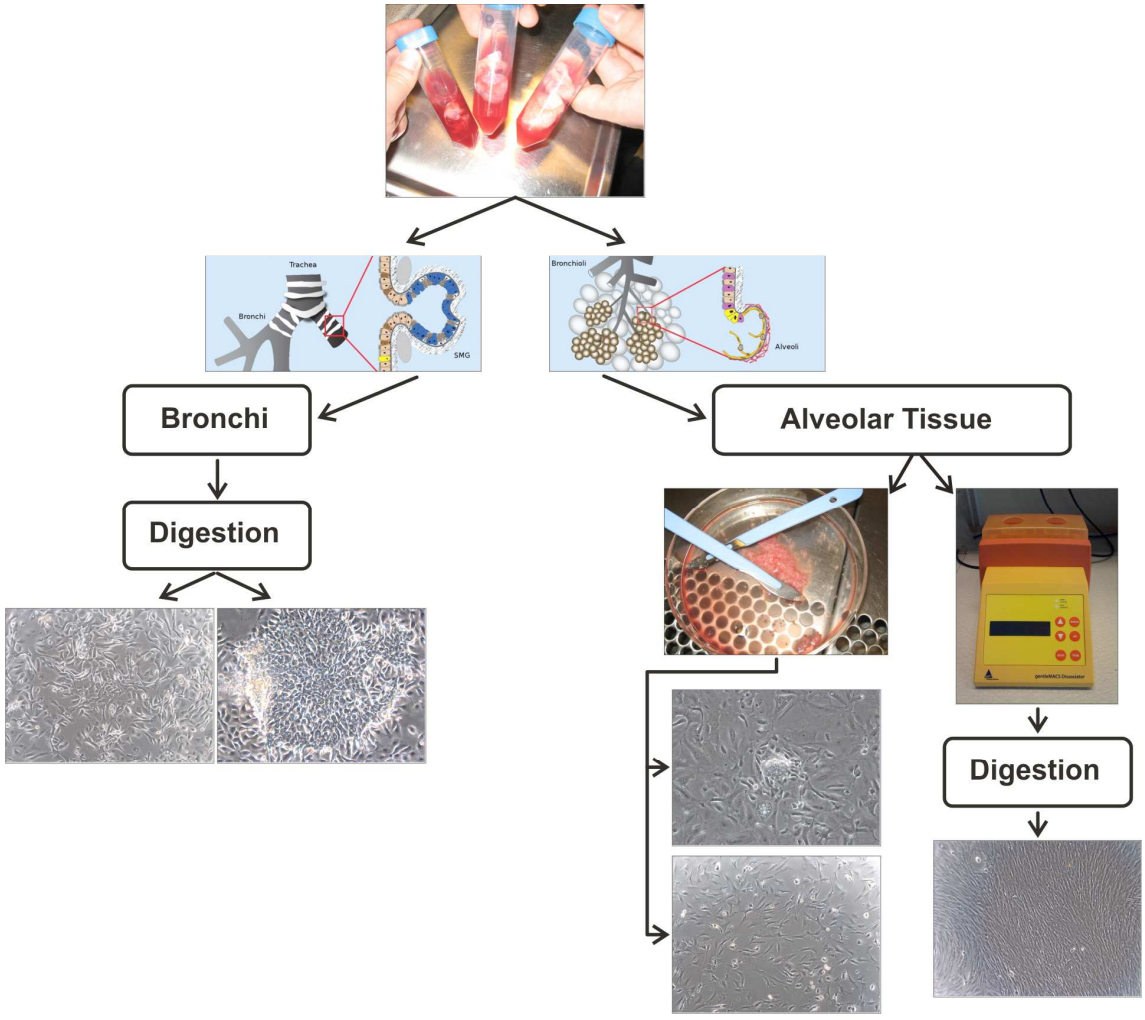

Figure 22: Examples of cell isolation from bronchial and alveolar lung tissue. Protocols for different areas of the lungs differ. Bronchial tissue is digested over night at 4°C and then seeded onto collagen coated culture flasks. Alveolar tissue is more difficult to deal with. Chopping (manually or by using the gentlaMACS dissociator) and/or digestion of alveolar tissue followed by seeding onto collagen coated surfaces results in alveolar fibroblast isolation.

Various isolation protocols are available incorporating many different enzymes and reagents. These methods are, however, not easily transferred from one laboratory to another. In this project current protocols have been modified and mostly relied on manual disintegration of the tissue followed by seeding of organoids onto cell culture flasks.

5.1.1 Bronchial cells

General cell isolation from bronchial tissue has turned out to be a fairly straightforward procedure. When cells are isolated, bronchial tissue is digested with either protease XVI or 0.1% Trypsin-EDTA/PBS for 48 hours at 4°C. Following digestion, the bronchial epithelium is isolated by manually scraping if off the bronchial cartilage using a sterile scalpel. This results in small organoids of bronchial tissue that adhere to collagen coated culture flasks and ultimately result in bronchial cell outgrowth from a central organoid (figure 22, left). These cells exhibit an epithelial cell marker expression when cultured in conventional monolayer cultures. The isolated cells are uniformly CK14, E-cadherin and EpCAM positive while being negative for the mesenchymal marker Thy1 (figure 23). In addition, it is common to see ciliated cells surrounding the organoids in culture for a few days after isolation. Direct seeding into conventional monolayer cultures does not seem to be the optimal method to facilitate stem cell enrichment in commonly isolated cells.

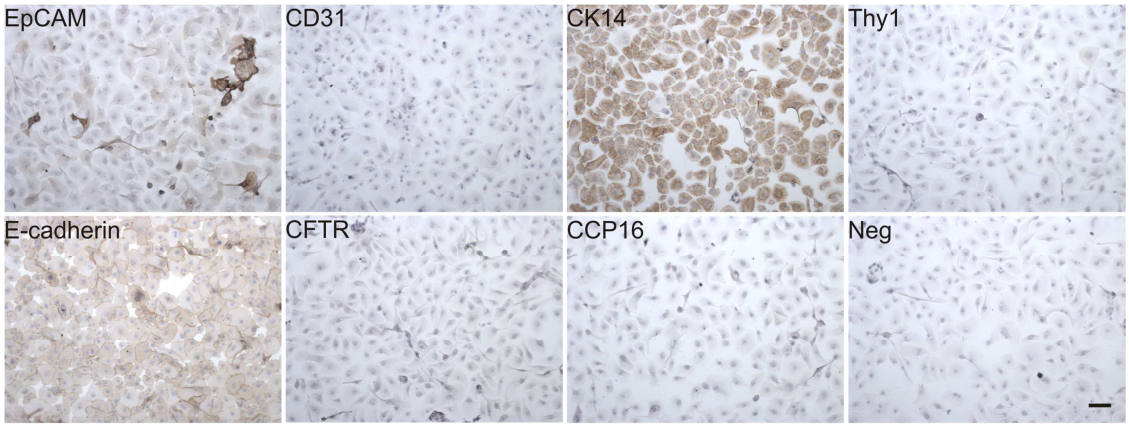

Figure 23: Primary bronchial cells express basal cell markers in monolayer culture. The most commonly isolated cells are EpCAM, CK14 and E-cadherin positive indicating a cell population comprised mainly of epithelial cells. No Clara cells or fibroblasts are commonly isolated. Bar 100μm.

5.1.2 Cells from alveolar regions

Cell isolation from the alveolar regions of the lung has proven to be more difficult and so far only primary fibroblasts have been isolated from distal tissue samples. In alveolar isolation the main focus has been on manual dissociation of the tissue rather than enzymatic digestion. Digestion with various enzymes could result in the isolation of different cells. Commonly collagenase is used to break up the ECM and facilitate isolation of the epithelial cells (Gudjonsson et al., 2002; Pechoux et al., 1999). In this project, the isolated cells were uniformly Thy1 positive indicating that this method is successful for the isolation of alveolar fibroblasts. Occasionally EpCAM positive cells are found in these cell cultures indicating that few epithelial cells can be isolated by this method. However, the current yield is nowhere near satisfactory (figure 24).

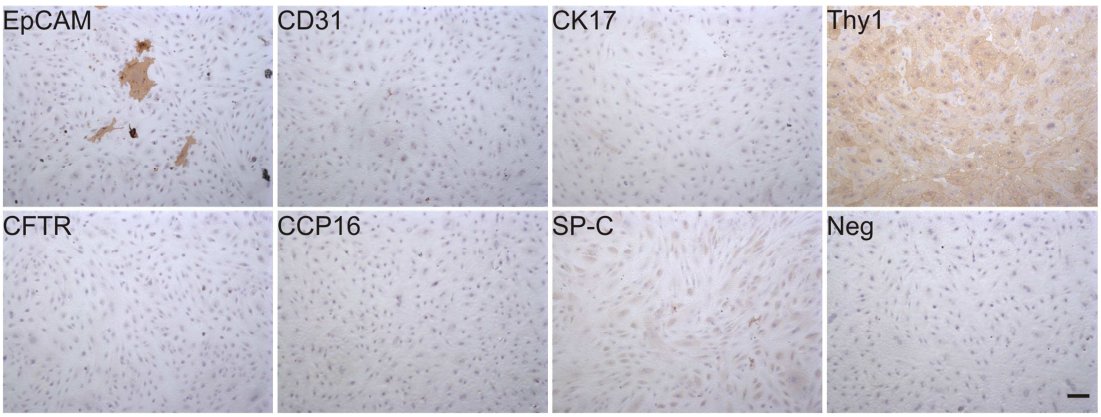

Figure 24: Chopping of alveolar tissue returns mainly Thy1 positive fibroblasts. The current method of simply disintegrating the tissue by chopping does not seem to facilitate the isolation of epithelial cells. However, it is optimal for the isolation of alveolar fibroblasts. Bar 100µm.

Table 7: Overview of cell isolations from primary tissue. Overview over number of biopsies and tissue type. Additionally, number of vials frozen along with cell passage number (P=passage) is also listed along with investigative assays performed on the isolated cells.

Biopsy	Date	Type	Vials Frozen	Assays
1	01.10.2010	Proximal/Distal	5xP4	DAB
2	12.10.2010	Distal	N/A	N/A
3	29.10.2010	Proximal/Distal	5xP3	DAB, UG, 3D
4	30.11.2010	Distal	N/A	DAB, MACS
5	07.01.2011	Proximal/Distal	3xP2, 5xP3	N/A
6	11.02.2011	Proximal/Distal	N/A	MACS
7	18.02.2011	Proximal/Distal	N/A	MACS
8	25.02.2011	Proximal/Distal	N/A	N/A
9	22.03.2011	Proximal/Distal	2xP5(d)	ALI, 3D, UG, IF, MACS
10	29.03.2011	Distal	2xP3(d)	MACS
11	01.07.2011	Proximal/Distal	2xP1	3D, MACS, ALI, IF
12	30.08.2011	Proximal/Distal	1xP3	LA, 3D, IF, UG, PI
13	25.10.2011	Proximal/Distal	1xP1	3D, MACS

6. Functional and phenotypic characterization of primary lung cells

6.1 Bronchial Cells

Isolated bronchial cells in 3D co-culture with endothelial cells form solid round colonies. Although, those colonies are somewhat smaller than the solid round colonies formed by VA10. In addition, unlike VA10 cells, they do not exhibit bronchioalveolar structures under these culture conditions.

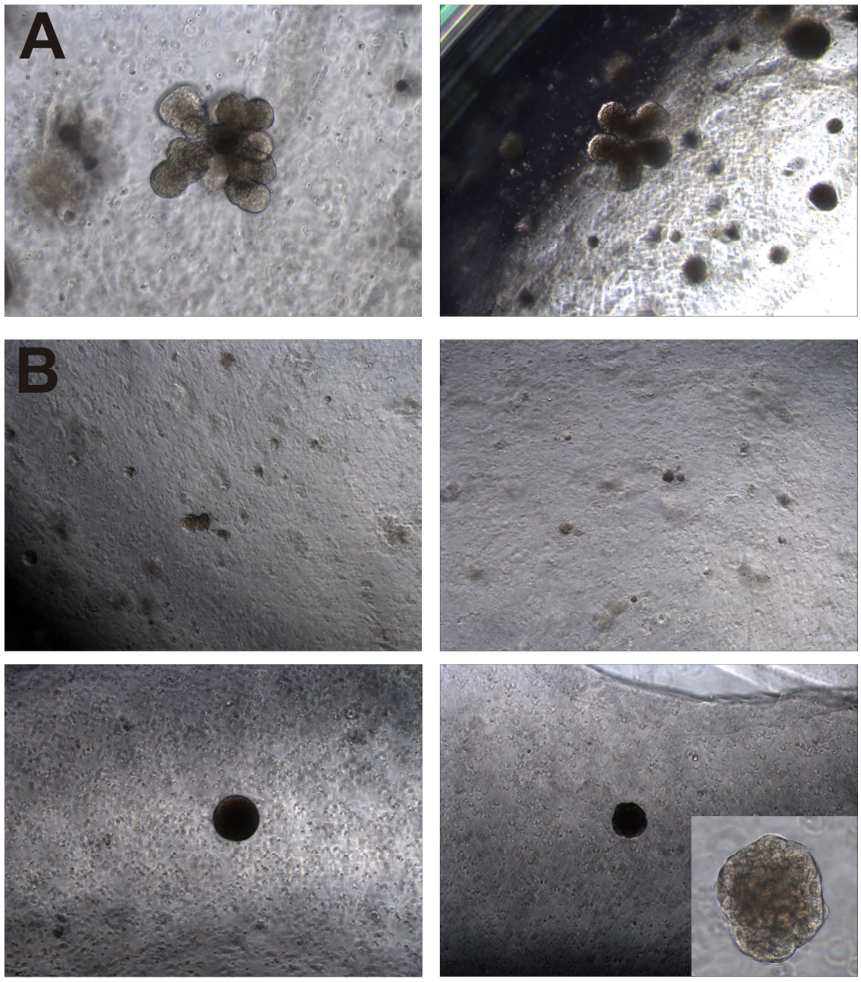

Figure 25: Isolated primary bronchial cells do not form bronchioalveolar-like structures in 3D cultures. A: Typical branching in VA10 co-cultured with HUVECs. **B:** Solid round colonies of primary bronchial cells in co-culture. Original magnification 5x. Inset, 20x magnification.

6.1.1 Bronchial cells show goblet cell differentiation in ALI cultures

When primary bronchial cells are cultured in the ALI culture system they exhibit both ciliated (70%) and goblet (30%) cell differentiation when cultured on traditional differentiation medium (DMEM+2%UG). VA10 does not show this goblet cell differentiation under the same conditions. They can, however, be induced to undergo goblet cell differentiation with IL-13 (Arason et al. unpublished results).

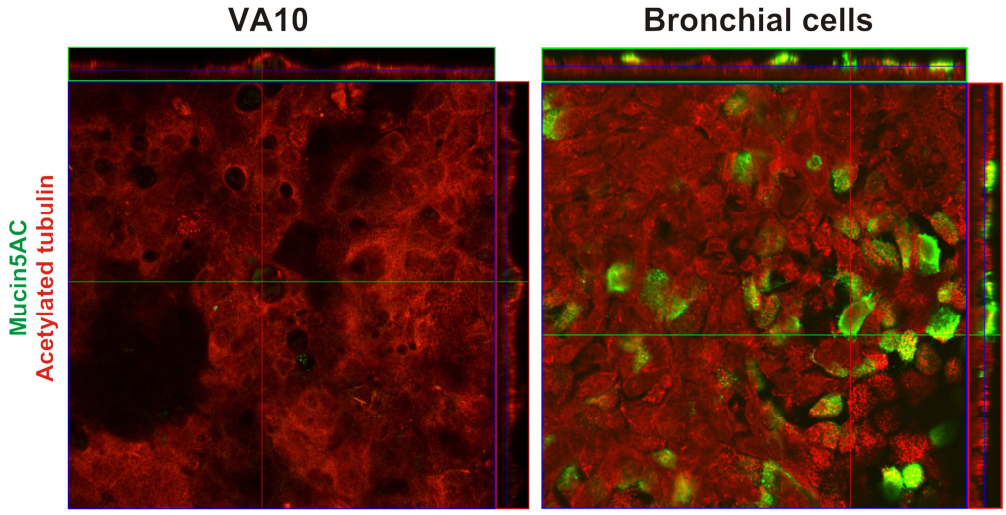

Figure 26: Isolated primary bronchial cells differentiate into goblet cells when cultured in air liquid interface cultures. Epithelial layers of primary bronchial cells contain both ciliated and goblet cells while VA10 epithelium only appears to contain ciliated cells. Original magnification 10x. This work was done in collaboration with Ari Jón Arason.

6.2 Alveolar fibroblasts in 3D cultures

Alveolar fibroblasts do not form colonies in three-dimensional cultures. They do, however, function quite well as feeder cells when cultured with VA10. Prior to seeding the fibroblasts are treated with Mitomycin C, a DNA crosslinking agent, in order to inhibit their growth and prevent them from interfering with the growth of the epithelial cells. VA10 cells in co-culture with alveolar fibroblasts form their characteristic bronchioalveolar-like structures, however, they are somewhat more irregular in shape than endothelial induced bronchioalveolar-like structures (figures 25A and 27).

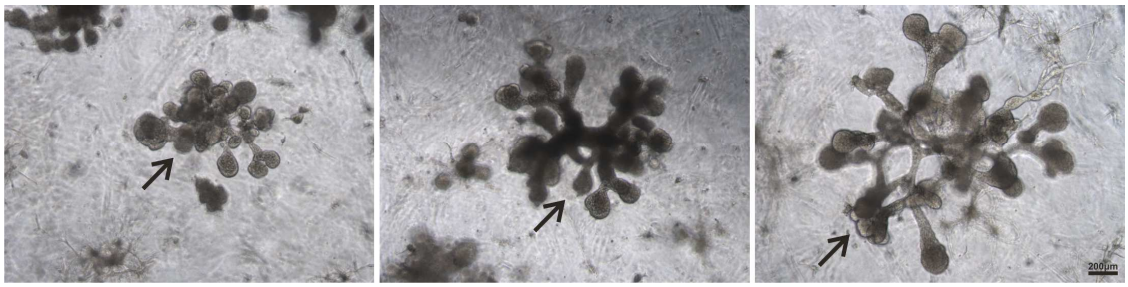

Figure 27: VA10 cells form their characteristic bronchioalveolar-like structures when co-cultured with primary alveolar fibroblasts (arrows). VA10 structures in fibroblast co-cultures are more irregular in shape than those formed in endothelial co-cultures. Bar 200µm.

Similar results were obtained on one occasion using isolated primary bronchial cells. The resulting structures were considerably smaller than those formed by VA10 under the same conditions (figure 28).

Figure 28: Primary bronchial cells form small bronchioalveolar-like structures in co-cultures with primary alveolar fibroblasts (arrows). In contrast, commonly isolated bronchial cells did not form bronchioalveolar structures in 3D co-cultures with endothelial cells. Bar 200µm.

7. Primary epithelial cells are refractory to EMT induction by Ultroser G

Primary bronchial epithelial cells do not exhibit the same subgroup distinction as VA10 when treated with Ultroser G (UG). These cells undergo less clear morphological changes when cultured on UG and co-express E-cadherin and Vimentin (figure 29, lower panel).

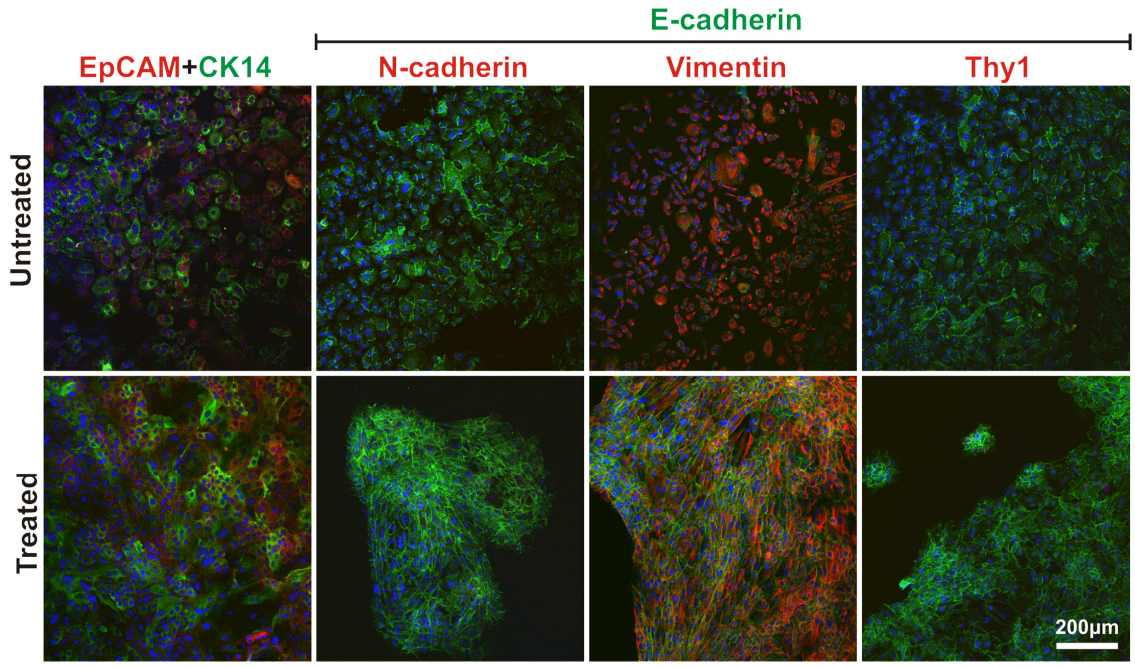

Figure 29: Primary bronchial cells do not exhibit the same subgroup distinction as VA10 cells when treated with Ultroser G. Bronchial cells respond to Ultroser G in a different way than VA10 cells. They grow much tighter and exhibit a higher expression of E-cadherin. E-cadherin and Vimentin are also co-expressed in these cells. Bar 200µm.

V – Discussion

1. Summary

In this thesis I have studied the marker expression of the epithelial and mesenchymal compartments in normal and fibrotic lung tissue *in situ* with focus on capturing the phenotype of epithelial-to-mesenchymal transition (EMT).

I have observed a distinct increase in CK14 positive basal cells in lung epithelium adjacent to fibrotic areas (fibroblastic foci) in samples from IPF patients. Additionally, the epithelium also shows a strong expression of Vimentin indicating a partial EMT in epithelial cells close to fibrotic foci. This indicates that the epithelium could possibly be contributing to fibrotic conditions in IPF.

Furthermore, to support my *in situ* studies, I have also analyzed the plasticity of human bronchial epithelial cell line (VA10) with basal cell characteristics and stem cell properties. When VA10 cells are propagated in monolayer in growth media supplemented with Ultroser G, conditions that commonly favor pseudostratified differentiation in air-liquid interface cultures, I observed phenotypic changes that gave rise to distinct islands of epithelial and mesenchymal cell populations. Using magnetic cell sorting based on negative selection of EpCAM positive cells followed by a positive selection of Thy1 expressing cells I was able to isolate the mesenchymal-like subgroup from VA10. These mesenchymal-like cells, referred to as VA10 $Thy1^{pos}$, no longer express selected epithelial markers but have gained a high expression of mesenchymal markers such as Vimentin, N-cadherin and Thy1. Additionally, these cells no longer exhibit branching potential in three-dimensional co-cultures with endothelial cells. Instead, they form disintegrated spindle-like colonies reminiscent of mesenchymal cells. This, along with down-regulation of miRNA200c, increased resistance to apoptosis and increased potential for anchorage independent growth, indicates that a subset of VA10 cells undergoes mesenchymal-to-epithelial transition when treated with Ultroser G in monolayer culture.

To evaluate whether EMT could also occur in primary bronchial cells I established protocols for isolation of epithelial cells from fresh human lung tissue. This was a time consuming and technically difficult task due to the individual difference between patient materials coupled with the challenge of acquiring enough of it. The isolation of bronchial cells was, however, more straightforward than isolation of cells from the alveolar regions. In my initial experiments with primary epithelial cells I have not observed any clear phenotypic plasticity towards EMT. However, this needs to be confirmed by experiments using primary cells isolated from more patients.

2. Idiopathic pulmonary fibrosis (IPF)

Idiopathic pulmonary fibrosis (IPF) is characterized by the formation of fibroblastic foci in lung tissue. These foci are composed of fibroblasts and myofibroblasts and will eventually cause a loss of function in the surrounding lung epithelium. This loss of function then causes severe respiratory distress and death in IPF patients (reviewed in (Hardie et al., 2010)).

2.1 EMT in IPF

The cellular origin of fibroblastic foci in IPF is currently unclear but recent studies have pinpointed epithelial-to-mesenchymal transition (EMT) of lung epithelial cells as a possible cellular source (Morbini et al., 2011). When normal lung tissue is compared to lung tissue of IPF patients there are observable changes in marker expression in the epithelium adjacent to fibroblastic foci. There is a clear up-regulation of Vimentin expression in epithelial cells surrounding fibroblastic foci compared to control samples (figures 7 and 8). This could indicate that EMT has occurred in these cells and they could possibly be contributing to fibrotic conditions. Interestingly, a marked increase in CK14 expression is also observed in these cells (figure 8). Since CK14 is rather expected to be down regulated in cells that have undergone EMT it could be speculated that this represents a growth increase in CK14 positive basal cells within foci adjacent pulmonary epithelium. Most studies that focus on EMT in pulmonary epithelial cells have emphasized alveolar type II epithelial cells as the culprit but it has been suggested that increased proliferation of basal epithelial cells at the bronchioalveolar junction may play a part in the pathogenesis of the disease (Chilosi et al., 2002). This is consistent with the observed increase in CK14 expression seen in IPF patient samples. Preliminary results also indicate an increase in the expression of the basal cell transcription factor p63 in the same subset of cells in IPF samples further strengthening this hypothesis (data not shown). In addition to the theory of EMT induced fibrosis it has also been speculated that resident fibroblasts of the lung could contribute to pulmonary fibrosis along with mesenchymal stem cells from the blood (Willis et al., 2006). When all of this is considered together it is quite possible that all these different cell types contribute in some way to the onset of fibrosis in the lungs. The specific role and importance of each of these cell types is, however, unclear. It is important to gain more knowledge about the pathogenesis of IPF in order to be able to properly understand the causes of this particular disease as well as other fibrotic pulmonary diseases (reviewed in (Hardie et al., 2010)).

3. Ultroser G induced EMT in VA10 cells

Epithelial-to-mesenchymal transition can be readily induced in various *in vitro* cellular systems. The most common method of induction involves Transforming Growth Factor β-1 (TGFβ-1) which induces EMT through the Smad signaling pathway (Phanish et al., 2006). Additionally, various chemical agents, such as Bleomycin, can also induce EMT (Alipio et al., 2011).

In contrast to A549, TGFβ-1 does not induce EMT in VA10 cells (data not shown). However, EMT in VA10 cells can be induced using the serum substitute Ultroser G (UG) that contains various undefined growth factors and larger proteins. Interestingly, only a subset of VA10 cells seems to be susceptible to EMT induced by UG as only a fraction of the cells undergo morphological changes when treated (figure 10A, arrows). The switch in marker expression is clear in these cells. They go from expressing predominantly epithelial markers (figure 9) to having a strong mesenchymal expression pattern (figure 12B, lower panel). It is currently unclear which factor in UG is responsible for these morphological changes in VA10. In 1991 Clerc et al. described a vague composition of UG mentioning both epithelial and fibroblast growth factors, along with insulin like growth factors, nerve growth factor, growth hormone, prolactin, colony stimulating factor, platelet derived growth factors, albumin, insulin, transferrin and lipids (Clerc et al., 1991). Any number of these growth factors could be involved in the phenotypic change of VA10 cells. In 1989, Boyer at al. showed reversible UG induced EMT in the rat carcinoma cell line NBT-II (Boyer et al., 1989). A few years later the same group determined that EMT could be induced in these same cells through fibroblast growth factor (FGF) signaling via different FGF receptors (Savagner et al., 1994). It is possible that something similar is happening to the VA10 cells in our model since the induced EMT phenotype is partially reversible simply by culturing the cells in the absence of UG (figure 21).

In order to confirm that these phenotypic changes in VA10 cells were caused by EMT I assessed the functional properties of the mesenchymal-like subgroup. This was done after the mesenchymal-like cells had been positively selected from UG treated VA10 cells using magnetic cell sorting (MACS) for Thy1 (figure 12B, lower panel). The $Thy1^{pos}$ cells no longer exhibit branching potential in three-dimensional culture, a characteristic of the original VA10 cell line, indicating a loss of stem cell traits (figure 15). More importantly, the mesenchymal-like cells display increased resistance to apoptosis (figure 20) as well as increased potential for anchorage independent growth and migration (figures 17 and 18). This is characteristic of cells that have undergone EMT. Assessed expression of microRNA 200c in mesenchymal-like VA10 cells further confirmed the transition. Additionally, the mesenchymal cells are $CD44^{high}/CD24^{low}$ expressing (figure 13), an expressional profile that has been associated with metastatic breast cancer stem cells (V. Sigurdsson et al., 2011). Recently, the EMT phenotype has also been linked to this profile in breast epithelial cells (Mani et al., 2008).

3.1 Mesenchymal-like VA10 cells as a model for IPF

In this study, I have established a pulmonary EMT model in our basal lung epithelial cell line. As previously mentioned, our cell line exhibits stem cell properties measured by its ability to form both pseudostratified epithelium and bronchioalveolar-like structures in culture (Franzdottir et al., 2010; Halldorsson et al., 2007). When this is put into context with cellular conditions in IPF this basal epithelial stem cell could possibly serve as an ideal target cell for EMT in IPF both due to its progenitor cell capabilities and potential for epithelial plasticity.

My *in vitro* mesenchymal model shares some characteristics with cells found in fibroblastic foci in idiopathic pulmonary fibrosis and the surrounding epithelium. This model could possibly contribute to our knowledge of pulmonary EMT and provide valuable insights into the pathogenesis of IPF.

4. Isolation of primary lung epithelial cells

In order to better captivate *in vivo* conditions in *in vitro* cultures it is important to have access to representative culture models. Many different cell lines are available but due to the fact that cell lines either have cancerous origin or have been manipulated to grow indefinitely in culture it is important to venture into the culture of primary cells isolated from normal tissue.

The human lung contains many different cell types. Some can be easily isolated while the isolation of others is more complicated (figure 22). In this project, a stable isolation protocol for bronchial cells has been established. These isolations mainly return E-cadherin and CK14 positive cells resembling the bronchial epithelial cell line, VA10 (figure 23). The isolated cells do not, however, undergo branching morphogenesis when cultured in three-dimensional co-cultures indicating that the current method of isolation does not enrich for bronchial cells possessing stem cell properties (figure 25). Isolated bronchial cells do, however, differentiate into both ciliated and goblet cells when cultured in the ALI system whereas VA10 cells primarily undergo ciliary differentiation (figure 26). In order to enrich for cells that possess stem cell properties it might be necessary to culture the isolated cells on fibroblast feeder cells. This was recently done using primary upper and lower airway epithelial cells (Kumar et al., 2011). This is also done with embryonic stem cells to keep them in a de-differentiated state (Pall et al., 2011; Yu et al., 2011). Additionally, it might be useful to analyze isolated cells by flow cytometry immediately after isolation and utilize various cell sorting techniques to sort out possible progenitor cell populations.

Isolation of cells from distal areas of the lung is made complex by close proximity of the alveolar epithelium and stromal tissue. In order to gain access to the epithelial cells the stromal tissue must be digested and disintegrated first. This is an intricate process involving many different enzymes and incubation times and temperatures. Additionally, tissue samples can be disintegrated with either mechanical or manual chopping. As previously described, alveolar fibroblasts can be isolated from distal lung samples by simple manual chopping of the tissue

(figure 23). On rare occasion, a few EpCAM positive cells were isolated using this method indicating limited potential for epithelial cell isolation (figure 24).

Isolated alveolar fibroblasts can induce branching in VA10 when co-cultured in three-dimensional gel cultures. However, the resulting bronchioalveolar-like structures are more irregular in shape than those induced in endothelial co-cultures (figure 27).

Better protocols for isolation of alveolar epithelial cells must be developed utilizing both enzyme digestion and chopping to obtain optimal results. Methods similar to those used for bronchial cells could then be utilized for the enrichment of alveolar progenitor cell growth.

Individual sample difference plays a large role when dealing with cell isolations from human biopsies. During the isolation part of this project, I have had to work around this. It is frustrating when established isolation protocols do not yield the same results after each isolation. This severely limits the reproducibility of obtained results.

4.1 Ultroser G treatment of primary bronchial cells

Interestingly, UG treatment of isolated primary bronchial cells does not cause the same clear mesenchymal phenotype observed in VA10 cells. Treated primary cells tend to form tightly packed islets of somewhat elongated cells that display high co-expression of E-cadherin and Vimentin (figure 29). This resistance to UG induced EMT could possibly be explained by the fact that current isolation protocols do not enrich for stem cell growth resulting in the isolation of epithelial cells with lesser potential for plasticity and therefore less susceptibility to EMT induced only by UG. It is possible that EMT could be induced in these cells by incorporating other known EMT inducing agents, such as TGFβ-1, as well as UG. Stem cell properties aside, it is not unexpected that normal epithelial cells from the lung do not exhibit as much plasticity as an immortalized cell line. In fact, it is to be expected. Therefore it is not surprising that it turns out to be harder to induce EMT in normal primary cells.

Both in the mouse breast epithelium as well as in human breast cancer there is a close connection between EMT and stem cell properties (Guo et al., 2012; Mani et al., 2008). Therefore, it is important to isolate basal stem cells from the human lung in order to be able properly investigate the role of stem cell properties in pulmonary EMT in relation to IPF.

VI – Future Perspectives

In order to be able to properly assess the relationship and similarity between IPF and post-EMT cells both *in situ* and *in vitro* it is important to fully evaluate the expression of EMT related factors, surface markers and transcription factors, in normal lung tissue as well as in samples from patients suffering from IPF. It would also be interesting to further evaluate the migratory potential of mesenchymal VA10 cells and determine whether they can migrate rigorously enough to penetrate the basal membrane and enter the mesenchymal compartment. Modeling the *in vitro* migratory mechanism in EMT could describe how epithelial cells migrate *in vivo* and participate in the formation of fibroblastic foci in IPF.

It would also be intriguing to investigate which factors in Ultroser G are responsible for epithelial-to-mesenchymal transition in VA10 cells along with analyzing the mechanism of EMT in these cells. This includes evaluating signaling through tyrosine kinase receptors, methylation of promoter regions of important transcription factors and adhesion molecules such as E-cadherin. Furthermore, emerging roles of microRNAs in IPF need to be explored in more detail.

Additionally, continuous work needs to be carried out to improve protocols for cultivation of primary lung epithelial cells. We need to develop protocols that maximize the yield of cells isolated from each biopsy. Additionally, it is important to be able to separate different subpopulations of cells, especially stem cells, and test for plasticity towards a mesenchymal phenotype in these different populations. In that regard, it is also very important to improve protocols to isolate alveolar epithelial cells and prevent contamination from resident alveolar fibroblasts.

In the near future it will also be important to have access to fresh tissue from IPF patients for cell isolation to be able to analyze the behavior of these cells *in vitro*.

In summary, I believe that my work has captured an important issue in the etiology of IPF. Furthermore, the combination of *in situ* data with *in vitro* research will, in my opinion, lead to increased understanding of the pathogenesis of IPF.

VII – Appendix

1. Buffers

1.1 TE buffer

10mM Tris

1mM EDTA (Triplex)

in distilled water

1.2 MACS buffer

0.5% Bovine Serum Albumin (BSA)

1 mM EDTA

0.09% Sodium azide

in PBS

1.3 RIPA buffer

50 mM Tris-HCl, pH 8.0

150 mM NaCl

1.0% Igepal CA-630

0.5% Sodium deoxycholate

0.1% sodium dodecyl sulfate

in distilled water

VIII – References

Acloque, H., Adams, M. S., Fishwick, K., Bronner-Fraser, M., & Nieto, M. A. (2009). Epithelial-mesenchymal transitions: the importance of changing cell state in development and disease. *J Clin Invest, 119*(6), 1438-1449.

Affolter, M., Bellusci, S., Itoh, N., Shilo, B., Thiery, J. P., & Werb, Z. (2003). Tube or not tube: remodeling epithelial tissues by branching morphogenesis. *Dev Cell, 4*(1), 11-18.

Alipio, Z. A., Jones, N., Liao, W., Yang, J., Kulkarni, S., Sree Kumar, K., Hauer-Jensen, M., Ward, D. C., Ma, Y., & Fink, L. M. (2011). Epithelial to mesenchymal transition (EMT) induced by bleomycin or TFG(b1)/EGF in murine induced pluripotent stem cell-derived alveolar Type II-like cells. *Differentiation, 82*(2), 89-98.

Barcellos-Hoff, M. H., Aggeler, J., Ram, T. G., & Bissell, M. J. (1989). Functional differentiation and alveolar morphogenesis of primary mammary cultures on reconstituted basement membrane. *Development, 105*(2), 223-235.

Blick, T., Hugo, H., Widodo, E., Waltham, M., Pinto, C., Mani, S. A., Weinberg, R. A., Neve, R. M., Lenburg, M. E., & Thompson, E. W. (2010). Epithelial mesenchymal transition traits in human breast cancer cell lines parallel the CD44(hi/)CD24 (lo/-) stem cell phenotype in human breast cancer. *J Mammary Gland Biol Neoplasia, 15*(2), 235-252.

Boyer, B., Tucker, G. C., Valles, A. M., Gavrilovic, J., & Thiery, J. P. (1989). Reversible transition towards a fibroblastic phenotype in a rat carcinoma cell line. *Int J Cancer Suppl, 4*, 69-75.

Carterson, A. J., Honer zu Bentrup, K., Ott, C. M., Clarke, M. S., Pierson, D. L., Vanderburg, C. R., Buchanan, K. L., Nickerson, C. A., & Schurr, M. J. (2005). A549 lung epithelial cells grown as three-dimensional aggregates: alternative tissue culture model for Pseudomonas aeruginosa pathogenesis. *Infect Immun, 73*(2), 1129-1140.

Chang, K. C., Wang, C., & Wang, H. (2012). Balancing self-renewal and differentiation by asymmetric division: Insights from brain tumor suppressors in Drosophila neural stem cells. *Bioessays, 34*(4), 301-310.

Chilosi, M., Poletti, V., Murer, B., Lestani, M., Cancellieri, A., Montagna, L., Piccoli, P., Cangi, G., Semenzato, G., & Doglioni, C. (2002). Abnormal re-epithelialization and lung remodeling in idiopathic pulmonary fibrosis: the role of deltaN-p63. *Lab Invest, 82*(10), 1335-1345.

Clerc, P., Bensaadi, N., Pradel, P., Estival, A., Clemente, F., & Vaysse, N. (1991). Lipid-dependent proliferation of pancreatic cancer cell lines. *Cancer Res, 51*(14), 3633-3638.

Colbert, B., Ankney, J., Lee, K., Steggall, M., & Dingle, M. (2009). *Anatomy and Physiology for nursing and health professionals*. Essex, England: Pearson Education Limited.

Dairkee, S. H., Blayney, C. M., Asarnow, D. M., Smith, H. S., & Hackett, A. J. (1985). Early expression of vimentin in human mammary cultures. *In Vitro Cell Dev Biol, 21*(6), 321-327.

Daum, N., Kuehn, A., Hein, S., Schaefer, U. F., Huwer, H., & Lehr, C. M. (2012). Isolation, cultivation, and application of human alveolar epithelial cells. *Methods Mol Biol, 806*, 31-42.

Demayo, F., Minoo, P., Plopper, C. G., Schuger, L., Shannon, J., & Torday, J. S. (2002). Mesenchymal-epithelial interactions in lung development and repair: are modeling and remodeling the same process? *Am J Physiol Lung Cell Mol Physiol, 283*(3), L510-517.

Eades, G., Yao, Y., Yang, M., Zhang, Y., Chumsri, S., & Zhou, Q. (2011). miR-200a regulates SIRT1 expression and epithelial to mesenchymal transition (EMT)-like transformation in mammary epithelial cells. *J Biol Chem, 286*(29), 25992-26002.

Eriksson, J. E., Dechat, T., Grin, B., Helfand, B., Mendez, M., Pallari, H. M., & Goldman, R. D. (2009). Introducing intermediate filaments: from discovery to disease. *J Clin Invest, 119*(7), 1763-1771.

Eroschenko, V. P. (2005). *diFiore's Atlas of Histology with Functional Correlations, 10th edition* Lippincott Williams & Wilkins.

Franzdottir, S. R., Axelsson, I. T., Arason, A. J., Baldursson, O., Gudjonsson, T., & Magnusson, M. K. (2010). Airway branching morphogenesis in three dimensional culture. *Respir Res, 11*, 162.

Fujino, N., Kubo, H., Ota, C., Suzuki, T., Suzuki, S., Yamada, M., Takahashi, T., He, M., Suzuki, T., Kondo, T., & Yamaya, M. (2011). A Novel Method for Isolating Individual Cellular Components from the Adult Human Distal Lung. *Am J Respir Cell Mol Biol*.

Giangreco, A., Arwert, E. N., Rosewell, I. R., Snyder, J., Watt, F. M., & Stripp, B. R. (2009). Stem cells are dispensable for lung homeostasis but restore airways after injury. *Proc Natl Acad Sci U S A, 106*(23), 9286-9291.

Giangreco, A., Groot, K. R., & Janes, S. M. (2007). Lung cancer and lung stem cells: strange bedfellows? *Am J Respir Crit Care Med, 175*(6), 547-553.

Gilbert, S. F. (1997). *Developmental Biology, 5th edition*. Massachusets: Sinauer Associates Inc.

Gregory, P. A., Bert, A. G., Paterson, E. L., Barry, S. C., Tsykin, A., Farshid, G., Vadas, M. A., Khew-Goodall, Y., & Goodall, G. J. (2008). The miR-200 family and miR-205 regulate epithelial to mesenchymal transition by targeting ZEB1 and SIP1. *Nat Cell Biol, 10*(5), 593-601.

Gudjonsson, T., & Magnusson, M. K. (2005). Stem cell biology and the cellular pathways of carcinogenesis. *APMIS, 113*(11-12), 922-929.

Gudjonsson, T., Ronnov-Jessen, L., Villadsen, R., Bissell, M. J., & Petersen, O. W. (2003). To create the correct microenvironment: three-dimensional heterotypic collagen assays for human breast epithelial morphogenesis and neoplasia. *Methods, 30*(3), 247-255.

Gudjonsson, T., Villadsen, R., Nielsen, H. L., Ronnov-Jessen, L., Bissell, M. J., & Petersen, O. W. (2002). Isolation, immortalization, and characterization of a human breast epithelial cell line with stem cell properties. *Genes Dev, 16*(6), 693-706.

Guo, W., Keckesova, Z., Donaher, J. L., Shibue, T., Tischler, V., Reinhardt, F., Itzkovitz, S., Noske, A., Zurrer-Hardi, U., Bell, G., Tam, W. L., Mani, S. A., van Oudenaarden, A., & Weinberg, R. A. (2012). Slug and sox9 cooperatively determine the mammary stem cell state. *Cell, 148*(5), 1015-1028.

Halldorsson, S., Asgrimsson, V., Axelsson, I., Gudmundsson, G. H., Steinarsdottir, M., Baldursson, O., & Gudjonsson, T. (2007). Differentiation potential of a basal epithelial cell line established from human bronchial explant. *In Vitro Cell Dev Biol Anim, 43*(8-9), 283-289.

Halldorsson, S., Gudjonsson, T., Gottfredsson, M., Singh, P. K., Gudmundsson, G. H., & Baldursson, O. (2010). Azithromycin maintains airway epithelial integrity during Pseudomonas aeruginosa infection. *Am J Respir Cell Mol Biol, 42*(1), 62-68.

Hardie, W. D., Hagood, J. S., Dave, V., Perl, A. K., Whitsett, J. A., Korfhagen, T. R., & Glasser, S. (2010). Signaling pathways in the epithelial origins of pulmonary fibrosis. *Cell Cycle, 9*(14), 2769-2776.

Hong, K. U., Reynolds, S. D., Watkins, S., Fuchs, E., & Stripp, B. R. (2004). Basal cells are a multipotent progenitor capable of renewing the bronchial epithelium. *Am J Pathol, 164*(2), 577-588.

Horowitz, A., & Simons, M. (2008). Branching morphogenesis. *Circ Res, 103*(8), 784-795.

Ingthorsson, I. (2008). *Modelling breast epithelial-endothelial interaction in three-dimensional culture.* University of Iceland, Reykjavík.

Kerosuo, L., & Bronner-Fraser, M. (2012). What is bad in cancer is good in the embryo: Importance of EMT in neural crest development. *Semin Cell Dev Biol*.

Korpal, M., Lee, E. S., Hu, G., & Kang, Y. (2008). The miR-200 family inhibits epithelial-mesenchymal transition and cancer cell migration by direct targeting of E-cadherin transcriptional repressors ZEB1 and ZEB2. *J Biol Chem, 283*(22), 14910-14914.

Kotton, D. N., & Fine, A. (2008). Lung stem cells. *Cell Tissue Res, 331*(1), 145-156.

Kumar, P. A., Hu, Y., Yamamoto, Y., Hoe, N. B., Wei, T. S., Mu, D., Sun, Y., Joo, L. S., Dagher, R., Zielonka, E. M., Wang de, Y., Lim, B., Chow, V. T., Crum, C. P., Xian, W., & McKeon, F. (2011). Distal airway stem cells yield alveoli in vitro and during lung regeneration following H1N1 influenza infection. *Cell, 147*(3), 525-538.

Lieber, M., Smith, B., Szakal, A., Nelson-Rees, W., & Todaro, G. (1976). A continuous tumor-cell line from a human lung carcinoma with properties of type II alveolar epithelial cells. *Int J Cancer, 17*(1), 62-70.

Lipkin, M., Sherlock, P., & Bell, B. M. (1962). Generation Time of Epithelial Cells in the Human Colon. [10.1038/195175b0]. *Nature, 195*(4837), 175-177.

Maeda, S., Suzuki, S., Suzuki, T., Endo, M., Moriya, T., Chida, M., Kondo, T., & Sasano, H. (2002). Analysis of intrapulmonary vessels and epithelial-endothelial interactions in the human developing lung. *Lab Invest, 82*(3), 293-301.

Magnusson, M. K., & Gudjonsson, T. (2011). Lung Epithelial Stem Cells. In K. Appasani & R. Appasani (Eds.), *Stem Cells & Regenerative medicine. From Molecular Embryology to Tissue Engineering*. New York, NY: Human Press.

Mani, S. A., Guo, W., Liao, M. J., Eaton, E. N., Ayyanan, A., Zhou, A. Y., Brooks, M., Reinhard, F., Zhang, C. C., Shipitsin, M., Campbell, L. L., Polyak, K., Brisken, C., Yang, J., & Weinberg, R. A. (2008). The epithelial-mesenchymal transition generates cells with properties of stem cells. *Cell, 133*(4), 704-715.

Mark, C., van Deurs, B., & Petersen, O. W. (1990). Regulation of vimentin expression in cultured human mammary epithelial cells. *Differentiation, 43*(2), 146-156.

Mauroy, B., Filoche, M., Weibel, E. R., & Sapoval, B. (2004). An optimal bronchial tree may be dangerous. *Nature, 427*(6975), 633-636.

Mendell, J. T., & Olson, E. N. (2012). MicroRNAs in Stress Signaling and Human Disease. *Cell, 148*(6), 1172-1187.

Mongroo, P. S., & Rustgi, A. K. (2010). The role of the miR-200 family in epithelial-mesenchymal transition. *Cancer Biol Ther, 10*(3), 219-222.

Morbini, P., Inghilleri, S., Campo, I., Oggionni, T., Zorzetto, M., & Luisetti, M. (2011). Incomplete expression of epithelial-mesenchymal transition markers in idiopathic pulmonary fibrosis. *Pathol Res Pract, 207*(9), 559-567.

Moustakas, A., & Heldin, C. H. (2007). Signaling networks guiding epithelial-mesenchymal transitions during embryogenesis and cancer progression. *Cancer Sci, 98*(10), 1512-1520.

Nakamura, M., & Tokura, Y. (2011). Epithelial-mesenchymal transition in the skin. *J Dermatol Sci, 61*(1), 7-13.

Pageau, S. C., Sazonova, O. V., Wong, J. Y., Soto, A. M., & Sonnenschein, C. (2011). The effect of stromal components on the modulation of the phenotype of human bronchial epithelial cells in 3D culture. *Biomaterials, 32*(29), 7169-7180.

Pall, E., Groza, I., Cenariu, M., Soritau, O., Gocza, E., & Tomuleasa, C. (2011). Establishment of an embryonic stem cell line from blastocyst stage mouse embryos. *Rom J Morphol Embryol, 52*(3 Suppl), 1005-1010.

Pechoux, C., Gudjonsson, T., Ronnov-Jessen, L., Bissell, M. J., & Petersen, O. W. (1999). Human mammary luminal epithelial cells contain progenitors to myoepithelial cells. *Dev Biol, 206*(1), 88-99.

Pellettieri, J., & Sanchez Alvarado, A. (2007). Cell turnover and adult tissue homeostasis: from humans to planarians. *Annu Rev Genet, 41*, 83-105.

Pezzulo, A. A., Starner, T. D., Scheetz, T. E., Traver, G. L., Tilley, A. E., Harvey, B. G., Crystal, R. G., McCray, P. B., Jr., & Zabner, J. (2011). The air-liquid interface and use of primary cell cultures are important to recapitulate the transcriptional profile of in vivo airway epithelia. *Am J Physiol Lung Cell Mol Physiol, 300*(1), L25-31.

Phanish, M. K., Wahab, N. A., Colville-Nash, P., Hendry, B. M., & Dockrell, M. E. (2006). The differential role of Smad2 and Smad3 in the regulation of pro-fibrotic TGFbeta1 responses in human proximal-tubule epithelial cells. *Biochem J, 393*(Pt 2), 601-607.

Radisky, D. C., & LaBarge, M. A. (2008). Epithelial-mesenchymal transition and the stem cell phenotype. *Cell Stem Cell, 2*(6), 511-512.

Reynolds, S. D., Giangreco, A., Power, J. H., & Stripp, B. R. (2000). Neuroepithelial bodies of pulmonary airways serve as a reservoir of progenitor cells capable of epithelial regeneration. *Am J Pathol, 156*(1), 269-278.

Rudnick, D. (1933). Developmental capacities of the chick lung in chorioallantoic grafts. *Journal of Experimental Zoology, 66*(1), 125-153.

Savagner, P. (2010). The epithelial-mesenchymal transition (EMT) phenomenon. *Ann Oncol, 21 Suppl 7*, vii89-92.

Savagner, P., Valles, A. M., Jouanneau, J., Yamada, K. M., & Thiery, J. P. (1994). Alternative splicing in fibroblast growth factor receptor 2 is associated with induced epithelial-mesenchymal transition in rat bladder carcinoma cells. *Mol Biol Cell, 5*(8), 851-862.

Shannon, J. M. (1994). Induction of alveolar type II cell differentiation in fetal tracheal epithelium by grafted distal lung mesenchyme. *Dev Biol, 166*(2), 600-614.

Shannon, J. M., & Hyatt, B. A. (2004). Epithelial-mesenchymal interactions in the developing lung. *Annu Rev Physiol, 66*, 625-645.

Shannon, J. M., Nielsen, L. D., Gebb, S. A., & Randell, S. H. (1998). Mesenchyme specifies epithelial differentiation in reciprocal recombinants of embryonic lung and trachea. *Dev Dyn, 212*(4), 482-494.

Shapiro, S. D. (2006). Animal models of asthma: Pro: Allergic avoidance of animal (model[s]) is not an option. *Am J Respir Crit Care Med, 174*(11), 1171-1173.

Sigurdsson, M. I., Isaksson, H. J., Gudmundsson, G., & Gudbjartsson, T. (2009). Diagnostic surgical lung biopsies for suspected interstitial lung diseases: a retrospective study. *Ann Thorac Surg, 88*(1), 227-232.

Sigurdsson, V., Hilmarsdottir, B., Sigmundsdottir, H., Fridriksdottir, A. J., Ringner, M., Villadsen, R., Borg, A., Agnarsson, B. A., Petersen, O. W., Magnusson, M. K., & Gudjonsson, T. (2011). Endothelial induced EMT in breast epithelial cells with stem cell properties. *PLoS One, 6*(9), e23833.

Thiery, J. P., Acloque, H., Huang, R. Y., & Nieto, M. A. (2009). Epithelial-mesenchymal transitions in development and disease. *Cell, 139*(5), 871-890.

Warburton, D., Schwarz, M., Tefft, D., Flores-Delgado, G., Anderson, K. D., & Cardoso, W. V. (2000). The molecular basis of lung morphogenesis. *Mech Dev, 92*(1), 55-81.

Ware, L. B. (2008). Modeling human lung disease in animals. *Am J Physiol Lung Cell Mol Physiol, 294*(2), L149-150.

Weinstein, G. D., McCullough, J. L., & Ross, P. (1984). Cell Proliferation in Normal Epidermis. *J Investig Dermatol, 82*(6), 623-628.

Willis, B. C., duBois, R. M., & Borok, Z. (2006). Epithelial origin of myofibroblasts during fibrosis in the lung. *Proc Am Thorac Soc, 3*(4), 377-382.

Yang, S., Banerjee, S., de Freitas, A., Sanders, Y. Y., Ding, Q., Matalon, S., Thannickal, V. J., Abraham, E., & Liu, G. (2012). Participation of miR-200 in Pulmonary Fibrosis. *Am J Pathol, 180*(2), 484-493.

Yu, Y. D., Kim, K. H., Lee, S. G., Choi, S. Y., Kim, Y. C., Byun, K. S., Cha, I. H., Park, K. Y., Cho, C. H., & Choi, D. H. (2011). Hepatic differentiation from human embryonic stem cells using stromal cells. *J Surg Res, 170*(2), e253-261.

Zabner, J., Karp, P., Seiler, M., Phillips, S. L., Mitchell, C. J., Saavedra, M., Welsh, M., & Klingelhutz, A. J. (2003). Development of cystic fibrosis and noncystic fibrosis airway cell lines. *Am J Physiol Lung Cell Mol Physiol, 284*(5), L844-854.

Zhang, Z., Zhang, B., Li, W., Fu, L., Fu, L., Zhu, Z., & Dong, J. T. (2011). Epigenetic Silencing of miR-203 Upregulates SNAI2 and Contributes to the Invasiveness of Malignant Breast Cancer Cells. *Genes Cancer, 2*(8), 782-791.

Zhu, Y., Chidekel, A., & Shaffer, T. H. (2010). Cultured human airway epithelial cells (calu-3): a model of human respiratory function, structure, and inflammatory responses. *Crit Care Res Pract, 2010*.